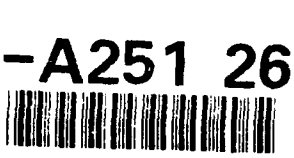

(2)

OFFICE OF NAVAL RESEARCH

GRANT N00014-90-J-1943

R&T Code 4134050

Technical Report No. 5

Collisions of $C_6H_6^{+\cdot}$, $C_6D_6^{+\cdot}$, $C_6H_5F^{+\cdot}$, $C_{60}^{+\cdot}$, and C_{60}^{++} at Fluorinated and Non-fluorinated Self-Assembled Monolayer Films

by

A. Somogyi, T.E. Kane, J.-M. Ding,
V.H. Wysocki, and J.H. Callahan

Prepared for Publication

in the

Journal of Physical Chemisty submitted

Virginia Commonwealth University
Department of Chemistry
Richmond, VA

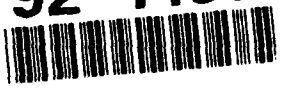

REPORT DOCUMENTATION PAGE

Form Approved
OMB No. 0704-0188

1. AGENCY USE ONLY (Leave blank)	2. REPORT DATE	3. REPORT TYPE AND DATES COVERED

4. TITLE AND SUBTITLE
Collisions of $C_6H_6^{+\cdot}$, $C_6D_6^{+\cdot}$, $C_6H_5F^{+\cdot}$, $C_{60}^{+\cdot}$, and C_{60}^{++} at Fluorinated and Non-Fluorinated Self-Assembled Monolayer Films

5. FUNDING NUMBERS
G N00014-90-J-1943

6. AUTHOR(S)
A. Somogyi, T.E. Kane, J.-M. Ding, V.H. Wysocki, and J.H. Callahan

7. PERFORMING ORGANIZATION NAME(S) AND ADDRESS(ES)
Department of Chemistry
Virginia Commonwealth University
Richmond, VA 23284-2006

8. PERFORMING ORGANIZATION REPORT NUMBER
5

9. SPONSORING/MONITORING AGENCY NAME(S) AND ADDRESS(ES)
Office of Naval Research
Chemistry Program
800 N. Quincy ST
Arlington, VA 22217

10. SPONSORING/MONITORING AGENCY REPORT NUMBER

11. SUPPLEMENTARY NOTES

12a. DISTRIBUTION/AVAILABILITY STATEMENT
Approved for public release
distribution unlimited

12b. DISTRIBUTION CODE

13. ABSTRACT *(Maximum 200 words)*

Mass spectra obtained by colliding singly-charged benzene, benzene-d_6 and fluorobenzene and singly- and doubly-charged buckminsterfullerene with self-assembled monolayer films are reported. These surfaces were prepared by the spontaneous assembly of C_2, C_3, C_4, C_{10}, and C_{18}, n-hydrocarbon thiols, perdeuteroeicosanethiol and 2-(perfluorooctyl)-ethanethiol on both gold foil and vapor-deposited gold are reported and discussed. The fluorinated surface provides the highest internal energy deposition; more extensive fragmentation of doubly-charged buckminsterfullerene could be observed on the other surfacces. Chemical reactions, such as H and CH_3 additions, as well as the analogue F and CF_3 additions, between benzene and fluorobenzene molecular ions and the monolayer films have been proved. These processes, ab initio 6-31G //6-31G SCF total energies and experimental heats of formation were used for the characterization of the surface-projectile interactions.

14. SUBJECT TERMS			15. NUMBER OF PAGES
			16. PRICE CODE
17. SECURITY CLASSIFICATION OF REPORT	18. SECURITY CLASSIFICATION OF THIS PAGE	19. SECURITY CLASSIFICATION OF ABSTRACT	20. LIMITATION OF ABSTRACT
unclassified	unclassified	unclassified	

GENERAL INSTRUCTIONS FOR COMPLETING SF 298

The Report Documentation Page (RDP) is used in announcing and cataloging reports. It is important that this information be consistent with the rest of the report, particularly the cover and title page. Instructions for filling in each block of the form follow. It is important to ***stay within the lines*** to meet ***optical scanning requirements***.

OFFICE OF NAVAL RESEARCH

Block 1. Agency Use Only *(Leave blank)*.

Block 2. Report Date. Full publication date including day, month, and year, if available (e.g. 1 Jan 88). Must cite at least the year.

N00014-90-J-1943

Block 3. Type of Report and Dates Covered. State whether report is interim, final, etc. If applicable, enter inclusive report dates (e.g. 10 Jun 87 - 30 Jun 88).

Block 4. Title and Subtitle. A title is taken from the part of the report that provides the most meaningful and complete information. When a report is prepared in more than one volume, repeat the primary title, add volume number, and include subtitle for the specific volume. On classified documents enter the title classification in parentheses.

Block 5. Funding Numbers. To include contract and grant numbers; may include program element number(s), project number(s), task number(s), and work unit number(s). Use the following labels:

C	- Contract	PR	- Project
G	- Grant	TA	- Task
PE	- Program Element	WU	- Work Unit Accession No.

Block 6. Author(s). Name(s) of person(s) responsible for writing the report, performing the research, or credited with the content of the report. If editor or compiler, this should follow the name(s).

Block 7. Performing Organization Name(s) and Address(es). Self-explanatory

Block 8. Performing Organization Report Number. Enter the unique alphanumeric report number(s) assigned by the organization performing the report.

Block 9. Sponsoring/Monitoring Agency Name(s) and Address(es). Self-explanatory.

Block 10. Sponsoring/Monitoring Agency Report Number. *(If known)*

Block 11. Supplementary Notes. Enter information not included elsewhere such as: Prepared in cooperation with...; Trans. of...; To be published in.... When a report is revised, include a statement whether the new report supersedes or supplements the older report.

Block 12a. Distribution/Availability Statement. Denotes public availability or limitations. Cite any availability to the public. Enter additional limitations or special markings in all capitals (e.g. NOFORN, REL, ITAR).

- **DOD** - See DoDD 5230.24, "Distribution Statements on Technical Documents."
- **DOE** - See authorities.
- **NASA** - See Handbook NHB 2200.2.
- **NTIS** - Leave blank.

Block 12b. Distribution Code.

- **DOD** - Leave blank.
- **DOE** - Enter DOE distribution categories from the Standard Distribution for Unclassified Scientific and Technical Reports.
- **NASA** - Leave blank.
- **NTIS** - Leave blank.

Block 13. Abstract. Include a brief *(Maximum 200 words)* factual summary of the most significant information contained in the report.

Block 14. Subject Terms. Keywords or phrases identifying major subjects in the report.

Block 15. Number of Pages. Enter the total number of pages.

Block 16. Price Code. Enter appropriate price code *(NTIS only)*

Blocks 17. - 19. Security Classifications. Self-explanatory. Enter U.S. Security Classification in accordance with U.S. Security Regulations (i.e., UNCLASSIFIED). If form contains classified information, stamp classification on the top and bottom of the page.

Block 20. Limitation of Abstract. This block must be completed to assign a limitation to the abstract. Enter either UL (unlimited) or SAR (same as report). An entry in this block is necessary if the abstract is to be limited. If blank, the abstract is assumed to be unlimited.

COLLISIONS OF $C_6H_6^{+\cdot}$, $C_6D_6^{+\cdot}$, $C_6H_5F^{+\cdot}$, $C_{60}^{+\cdot}$, AND C_{60}^{++} AT FLUORINATED AND NON-FLUORINATED SELF-ASSEMBLED MONOLAYER FILMS

Á. Somogyi[+], T.E. Kane, J.-M. Ding, and V.H. Wysocki[*]
Department of Chemistry, Virginia Commonwealth University, Richmond, VA 23284

J.H. Callahan
Chemistry Division, Naval Research Laboratory, Washington, DC, 20375

[+] On leave from Central Research Institute for Chemistry of the Hungarian Academy of Sciences, H-1525 Budapest, P.O.Box 17, Hungary.

[*] Author to whom correspondence should be addressed.

ABSTRACT

We report here the spectra that result when ionized benzene, ionized benzene-d_6, ionized fluorobenzene, and singly- and doubly-charged buckminsterfullerene collide with self-assembled monolayer films at collision energies ranging from 20-70 eV. The surfaces were prepared by the spontaneous assembly of C_2, C_3, C_4, C_{10} and C_{18} n-alkanethiols, perdeuteroeicosanethiol, and 2-(perfluorooctyl)-ethanethiol on both gold foil and vapor-deposited gold. Chemical reactions between the benzene molecular ion and the monolayer films are illustrated (e.g., H and CH_3 additions, F and CF_3 additions) and are shown to be sensitive to the chain length of the alkanethiolate. The fluorinated surface causes the greatest conversion of kinetic energy into internal energy; more extensive fragmentation of doubly-charged buckminsterfullerene is detected than is detected following collisions with the other surfaces. The experimental results, ab initio 6-31G*//6-31G SCF total energies, and experimental heats of formation were used for the characterization of the surface-projectile interactions.

INTRODUCTION

Collisions of mass-selected polyatomic ions with a surface promote extensive, structurally-characteristic fragmentation of the selected ion in an experiment referred to as surface-induced dissociation, SID.[1-18] Ion/surface reactions and chemical sputtering may also occur. The relative contribution of these competitive processes depends on both the nature of the projectile and the nature of the surface. Recently, self-assembled monolayer films were shown to be effective surfaces for ion/surface collisions.[17,18] These modified surfaces are prepared by the spontaneous assembly of 1-alkanethiols on gold[19-32] or silver[24] to form highly-ordered, covalently-bound monolayer films. Self-assembled monolayer films[19-36] are stable, easy to prepare, and useful for the electrochemical properties[26-32] they impart to electrode surfaces. Preliminary communications describing the use of these films as surfaces for ion/surface collision experiments illustrated that they greatly decrease the amount of chemical sputtering, as compared with untreated metals. They also provide a well-characterized surface for the investigation of ion/surface reactions.[17,18] We report here the spectra that result when ionized benzene, ionized benzene-d_6, ionized fluorobenzene, and singly- and doubly-charged buckminsterfullerene collide with self-assembled monolayer films. The monolayer surfaces were prepared from (i) alkanethiols of different (normal C_2, C_3, $C4_4$, C_{10} and C_{18}) chain lengths), (ii) perdeuteroeicosanethiol, and (iii) 2-(perfluorooctyl)-ethanethiol on gold foil and vapor-deposited gold. A fluorinated film was illustrated by Cooks and coworkers to eliminate ion/surface reactions with pyrazine, to increase the total scattered ion abundance, and to increase the total energy deposited into the projectile ion.[17] Fluorocarbons have higher ionization energies than hydrocarbons; this has the expected benefit of decreasing neutralization of projectile ions at the fluorinated surface compared to the hydrocarbon

surface.

Benzene was chosen for investigation because previous reports[1,4,5] indicate that a methyl addition reaction, with subsequent H_2 loss, occurs between benzene radical ions and adventitious hydrocarbons adsorbed on metal surfaces. When benzene was investigated on stainless steel in our laboratory, we detected not only the methyl addition reaction, but also additions of alkyl groups larger than methyl. Corresponding reactions (e.g., addition of C_nH_m, $n>1$) have been reported for larger aromatic hydrocarbons such as naphthalene, phenanthrene and pyrene.[1-3,15] The absence of surface reactions between pyrazine and a fluorinated surfaces noted by Cooks and coworkers suggested[17] that the ion-surface reaction chemistry of benzene could be different at a fluorinated surface; study of such interactions with the relatively well-characterized benzene system would provide further insight into the mechanisms of ion surface reactions.

Because Cooks and coworkers noted that energy deposition was higher for the fluorinated surfaces, we have also chosen to study the surface collision behavior of buckminsterfullerene. Buckminsterfullerene is considerably more difficult to fragment than smaller aromatic compounds. In their early studies of fullerenes, Smalley and coworkers showed that the fullerenes fragment by loss of C_2 or multiples of C_2; they used photodissociation tandem mass spectrometry to estimate that deposition of 18 eV was necessary to cause initial C_2 loss (on the microsecond time scale)[37]. The discovery of a synthetic technique for the bulk synthesis of buckminsterfullerene[38] has led to many subsequent studies of the fragmentation behavior of the fullerenes.[15] Several investigators[40-41] have also studied collisions of fullerene ions with surfaces of various types. These studies have shown that relatively high surface collision energies are necessary to fragment C_{60}^+, consistent with the relatively high activation energy for C_2

loss estimated by Smalley and coworkers.[37]

The objective of this work is to determine the influence of the nature of the surface on the extent of fragmentation of the projectile ions and on the type(s) of ion/surface reaction products detected. In addition to the spectra of benzene, benzene-d_6, and buckminsterfullerene, the surface-induced dissociation spectra of fluorobenzene are presented to explain fragmentation pathways for benzene ions that have added fluorine upon collision with the fluorinated surface. The results of *ab initio* (6-31G*//6-31G SCF) quantum mechanical calculations on a model system [benzene molecular ion plus CF_3CF_3] are used in conjunction with experimental heats of formation to help reveal features of the mechanism of reaction between benzene and a fluorinated surface. Collisions at the fluorinated surface are shown to result in more extensive projectile ion fragmentation and greater total scattered ion abundances than collisions at the hydrocarbon surface, in agreement with Cooks work.[17] This effect is especially pronounced for the doubly-charged buckminsterfullerene ion.

RESULTS AND DISCUSSION

Spectra of benzene and benzene-d_6 with hydrocarbon surfaces.

Figure 1 shows the spectra obtained for 30 and 70 eV collisions of the benzene molecular ion (m/z 78) with a surface prepared from octadecanethiol. The spectra show the expected[42] dissociation products of benzene (Table 1) but also show ions that result from ion surface reactions, e.g., m/z 91 and its fragment, m/z 65. An ion corresponding to H-addition is also evident (m/z 79). The ions at m/z 91 and 65 were also detected by Cooks and coworkers[1,4,5] for experiments performed on stainless steel and other surfaces and were suggested to correspond to addition of a methyl group followed by loss of H_2

and then loss of C_2H_2 (Scheme I).

SCHEME I

$$C_6H_6 + CH_3 \dashrightarrow C_7H_9 \quad (93) \quad \xrightarrow{-H_2} \quad C_7H_7 \quad (91) \quad \xrightarrow{-C_2H_2} \quad C_5H_5 \ (65)$$

To further explore the reaction in Scheme I, we obtained spectra for the reaction of ionized benzene and ionized benzene-d_6 with self-assembled monolayer films prepared from octadecanethiol and perdeuteroeicosanethiol; the appropriate reaction regions are illustrated in Figure 2. The peaks of interest shift by an appropriate number of mass units to confirm reaction with the self-assembled monolayer film and are consistent with an initial methyl addition. For ionized benzene reacting with the perdeutero surface (Scheme IIa; Figure 2a), the major products correspond to addition of CD_3 followed by loss of D_2 and loss of HD. For benzene-d_6 reacting with the octadecanethiol surface (Scheme IIb; Figure 2b), two predominant ions are present that correspond formally to a C_1 addition. These ions are m/z 96 and m/z 97, which are consistent with addition of CH_3 followed by loss of H_2 or HD. The loss of acetylene (C_2H_2, C_2HD, and C_2D_2) from these ions leads to the detected cluster of ions at m/z 68-70. For reaction between C_6D_6 and the perdeutero surface, the predominant reaction product corresponds to addition of CD_3 followed by loss of D_2 (Scheme IIc; Figure 2c).

SCHEME IIa

$$C_6H_6 + CD_3 \dashrightarrow C_7H_6D_3\ (96)$$

$$C_7H_6D_3 \xrightarrow{-H_2} C_7H_4D_3\ (94) \xrightarrow{-C_2H_2} C_5H_2D_3\ (68)$$
$$\xrightarrow{-C_2HD} C_5H_3D_2\ (67)$$
$$\xrightarrow{-C_2D_2} C_5H_4D\ (66)$$

$$C_7H_6D_3 \xrightarrow{-HD} C_7H_5D_2\ (93) \xrightarrow{-C_2H_2} C_5H_3D_2\ (67)$$
$$\xrightarrow{-C_2HD} C_5H_4D\ (66)$$
$$\xrightarrow{-C_2D_2} C_5H_5\ (65)$$

SCHEME IIb

$$C_6D_6 + CH_3 \dashrightarrow C_7D_6H_3\ (99)$$

$$C_7D_6H_3 \xrightarrow{-H_2} C_7D_6H\ (97) \xrightarrow{-C_2HD} C_5D_5\ (70)$$
$$\xrightarrow{-C_2D_2} C_5D_4H\ (69)$$

$$C_7D_6H_3 \xrightarrow{-HD} C_7D_5H_2\ (96) \xrightarrow{-C_2H_2} C_5D_5\ (70)$$
$$\xrightarrow{-C_2HD} C_4D_4H\ (69)$$
$$\xrightarrow{-C_2D_2} C_5D_3H\ (68)$$

SCHEME IIc

$$C_6D_6 + CD_3 \dashrightarrow C_7D_9\ (102) \xrightarrow{-D_2} C_7D_7\ (98) \xrightarrow{-C_2D_2} C_5D_5\ (70)$$

Long-chain alkane thiols are known to form more highly-ordered, crystalline surfaces than short-chain alkane thiols.[21] It was therefore desirable to determine whether ion/surface collision spectra vary with the chain length of the alkanethiol used to prepare the self-assembled monolayer film. Spectra were obtained on 6 different 'hydrocarbon' surfaces: untreated stainless steel and self-assembled monolayers prepared from ethanethiol, propanethiol, butanethiol, decanethiol, and octadecanethiol. The spectra are similar, but not identical, and appear to be sensitive to the nature of the surface (see Table 2). Spectra obtained for 30 eV and 70 eV collisions of ionized benzene with the C_{10} surface are illustrated in Figure 3. The spectra of Figure 3 are representative of the spectra obtained for stainless steel, and for the C_2, C_3, and C_4-alkanethiols but are

different from the spectrum obtained on the longer chain C_{18}-thiol (Figure 1). The differences between the spectra of Figures 1 and 3 can be illustrated by (i) the variation in the ratio of m/z 78 and m/z 77, (ii) the percent relative abundance of the ions at m/z 43 and 57, and (iii) the ratio of ions that correspond to addition of methyl and addition of ethyl (see Table 2).

Selected results for benzene-d_6 help explain the ratio of m/z 78 to m/z 77 for C_6H_6. The ion at m/z 77 in the spectrum of C_6H_6 could have more than one "parent" ion. Two likely precursors are [m/z 78 -H] and [m/z 79 -H_2]. Based on experimental heats of formation,[45] the heats of the H loss from the benzene molecular ion [$M^{+\cdot}$] and H_2 loss from the $[M+H]^+$ ion are 91.8 kcal/mol and 68.8 kcal/mol, respectively, which indicate the preference for the latter. The experimental data show that both processes occur. In agreement with the energetic prediction, data for benzene-d_6 suggest that a major formation pathway for the ion at m/z 77 in the spectrum of C_6H_6 is loss of H_2 from the H-addition ion, m/z 79 (Scheme III). For C_6D_6 (m/z 84), the appearance of an ion at m/z 81 cannot be explained by a direct loss of D or D_2 and must involve an initial H addition to C_6D_6 as suggested in Scheme III. The reaction of ionized benzene with the perdeutero surface yields the identical conclusion. The ratio of [(m/z 77)/(m/z 78)] is thus an indicator of the H-donating ability or H-reactivity of the surface. This ratio is greater than unity in cases of stainless steel and C_2-C_{10} hydrocarbon surfaces but less than unity for the C_{18} hydrocarbon surface (Table 2). This suggests that the amount of H-addition that is detected when benzene collides with the self-assembled monolayer film may be sensitive to the degree of surface 'disorder' or to the amount of adventitious hydrocarbon adsorbed at the surface.

The relative abundances of the ion at m/z 43 and m/z 57 are also of interest.

These ions cannot be direct dissociation products of $C_6H_6^{+\cdot}$ because they contain 7 hydrogens ($C_3H_7^+$) and 9 hydrogens ($C_4H_9^+$), respectively.[46] The m/z 43 ions are either dissociation products of m/z 79, the H-addition product of benzene, or alkyl ions that are sputtered from the surface. The relative abundance of m/z 43 is $\leq$ 0.1 % when the C_{18} thiol surface is used, but approximately 2-3% when the shorter-chain surfaces are investigated (Table 2). The ion of m/z 57 is either a dissociation product of a higher-order adduct (e.g., $[C_6H_6+CH_3]^+$ -> $C_4H_9^+$] or an alkyl ion that is sputtered directly from the surface. The formation of $C_3H_7^+$ (m/z 43) from $C_6H_7^+$ or $C_4H_9^+$ (m/z 57) from $C_7H_9^+$ would require extensive skeletal reorganization, suggesting that this pathway is unlikely. It seems more reasonable that the ions are the result of chemical sputtering of either the hydrocarbon chain of the alkane thiolate or adventitious hydrocarbons adsorbed onto the chemisorbed alkanethiolate film. The possibility that adventitious hydrocarbons are adsorbed onto, or inserted into, the films prepared from the shorter chain thiols ($\leq C_{10}$) is supported by the detection of m/z 57 ($C_4H_9^+$) when benzene collides with the C_2-thiol surface; $C_2H_5^+$ would be the largest alkyl ion that can be directly sputtered from the thiolate chain. Note that the relative abundances of ions at m/z 43 and 57 are $\leq$ 0.1 % when ionized benzene collides with the C_{18} thiol surface or the perdeutero-C_{20} surface.

The results for the alkyl addition to benzene also appear to indicate either the amount of "disorder" of the surface or the amount of adventitious hydrocarbon adsorbed. For the C_{18} surface, the ratio of methyl addition to ethyl addition is greater than for the other surfaces examined (compare Figures 1a and 3a; ratio of [89+91]/[103+105]). At a collision energy of 30 eV, this ratio decreases from greater than 50:1 for the C_{18} to approximately 10:1 on the other (C_{10}, C_4, C_3, C_2, stainless steel, and untreated gold) surfaces investigated. A possible explanation for this is that the more C_{18} surface

exposes mainly methyl groups for reaction with the incoming projectiles. The shorter-chain, more "dis" alkane thiol surfaces have more gauche interactions and also allow the addition of ethyl. Another possibility is that more adventitious hydrocarbon is accessible on the less- surface.

We suggest that fragmentation of the higher mass adducts (e.g., the ion corresponding to ethyl addition) can contribute to the ion abundance at m/z 91 (formal methyne addition, + CH_3 - H_2= + CH). Fragmentation of m/z 91 and adducts of higher mass also contributes to the ion abundances in the low mass portion of the spectrum. For example, the ion of m/z 27 that is detected in the 70 eV dissociation spectrum obtained upon collision of ionized deuterobenzene with the C_{18} thiol surface contains 3 hydrogens[43] and cannot result simply from fragmentation of $C_6D_6^{+\cdot}$ (see Table 1)[38]. Gas-phase experiments support the view that the formal CH addition can arise from addition of larger alkyl groups. If benzene is added to a chemical ionization plasma of isobutane (neutral benzene reacting with ionized hydrocarbon), adducts are formed that correspond to alkyl ion addition to benzene.[39] If one of these adducts, such as $[C_6H_6 + C_3H_7]^+$, is then mass-selected and allowed to collide with a target gas (Ar) or a surface, a fragment ion of m/z 91 is detected. Ionized benzene is known to be relatively unreactive with alkanes[44]; however, the above gas-phase experiments show that reaction products such as m/z 91 can be formed from adducts which formally consist of neutral benzene and an alkyl ion. These observations support the suggestion of Cooks and coworkers that the incoming benzene radical ion gains an electron and then adds an alkyl cation[1,4,5].

Based on the data described above, the octadecanethiol surface produces surface-induced dissociation spectra that have fewer contributions from competitive processes than do the other alkane thiol surfaces and untreated metal surfaces.

Although the relative amounts of H-addition, C_n ($n \geq 2$) addition, and chemical sputtering are greatly reduced at this surface, there are ions corresponding to H- and methyl addition. For some projectiles it is desirable to eliminate these products. For this reason, surfaces with no accessible hydrogens are being sought. One possibility is a fluorinated surface, as described below.

Spectra of benzene, benzene-d_6 and fluorobenzene with fluorinated alkanethiol surfaces.

A self-assembled monolayer prepared from 2-(perfluorooctyl)-ethane thiol was prepared with the expectation that H addition and CH_3 addition would not be accessible upon collisions of projectiles with this surface. The high ionization energies of fluorocarbons also lead to the expectation that neutralization should be decreased, compared with the hydrocarbon surfaces because charge exchange between the projectile ion and the fluorocarbon is not favorable energetically (IE benzene 9.25[47]; IE fluorocarbon, (e.g., C_3H_8) 13.38)[47]. This effect was illustrated by Cooks and coworkers for collisions of pyrazine with a fluorinated surface.[17] The SID spectra of the benzene molecular ion (m/z 78) colliding with the fluorinated surface at collision energies of 30 and 70 Ev are given in Figure 4. At a given collision energy, the relative abundance of low mass fragments is greater than is detected for ions colliding with the hydrocarbon surfaces (see e.g., Figure 1), suggesting that greater energy is deposited upon collision with the fluorinated surface. As expected, the intensities of the fragments having lower masses, i.e., higher energy requirements for dissociation, increase with increasing collision energy (see e.g., the intensity ratios of peaks at m/z 50:51, 38:39, 26:27) and the molecular ion is almost negligible at higher (greater than 50 eV) collision energies. Note that such an abundant fragment ion at m/z 26 in Figure 4 is not observed in the spectra

obtained by collision of ionized benzene with hydrocarbon surfaces (Figures 1 and 3). Furthermore, the efficiency, which is related to the total scattered ion abundance (see experimental), was found to improve significantly when the fluorinated surface, rather than the hydrocarbon surface, was used (ca. 30% vs. 2%, respectively; 30 eV collision energy). In addition to measuring the total ion current at the detector, a picoammeter is used to continuously measure the current at the surface while the experiment is in progress. Our results for total current measured at the surface agree qualitatively with the results of electrochemical studies.[25] Those monolayers that are the best blockers of electron transfer in solution (e.g. the fluorinated surface) give the lowest measured currents at the surface.

The appearance of the peaks at m/z 96 and m/z 95 (Figure 4) and m/z 127 (not shown) are also important. The origin of these peaks is most readily explained by assuming reaction between the benzene molecular ion and the perfluorinated chain of the surface; the formation of ions of m/z 96 and 95 can be initiated by fluorine addition followed by loss of H and H_2, respectively, while the formation of m/z 127 can be initiated by CF_3 addition, followed by the loss of HF. These assumptions are supported by the measurements made with benzene-d6; the peaks listed above are shifted to m/z 101, 99 and 132, respectively. The approximately 1:1 intensity ratio of the peaks at m/z 96 : 95 (Figure 4a) is significantly different from that observed in the fluorobenzene SID spectrum (Fig. 5), in which the above ratio is about 3. This difference in the m/z 96:95 ratio suggests that the peak at m/z 95 in the benzene SID spectrum does not result mainly from the H loss process from the fluorobenzene molecular ion (m/z 96). This latter process seems to be energetically unfavorable, since the intensity of the $[M-H]^+$ ion is quite low, even at 30 eV collision energy in the fluorobenzene SID spectrum (Figure 5).

Although only a very weak peak is observed at m/z 97 for reaction of benzene at the fluorinated surface (Figure 4a), it is reasonable to assume that the peak at m/z 95 is due to the loss of H_2 from the $[benzene+F]^+$ adduct, by analogy with the loss of H_2 from the $[benzene+CH_3]^+$ adduct discussed above.[1,4,5] We note here that *ab initio* calculations and experimental heats of formation (see below) indicate that this latter process is much more favorable energetically than the H loss from the molecular ion of fluorobenzene.

It is seen in a comparison of Figures 4 and 5 that the peaks at e.g. m/z 50, 39, 38, 27, 26 are present in both the benzene and fluorobenzene spectra. Because one can find the fluorobenzene molecular ion in the benzene spectra (Figure 4), it cannot be excluded that some percentage of these lower mass fragments originate from the fragmentation of the ion/surface reaction product, fluorobenzene, and not from the benzene molecular ion. This assumption is supported by the presence of the peaks at m/z 70, 57, and 45 in the benzene spectra (Figure 4), and by their shifts to m/z 73, 59, and 47, respectively, for the deuterated analogues. These ions can be interpreted as the "fluorinated" analogues of the fragments C_4H_4, C_3H_3 and C_2H_3, i.e. C_4H_3F, C_3H_2F and C_2H_2F, respectively. The peak at m/z 31 in the benzene SID spectra presumably corresponds to the ion CF^+. The relative abundances of the fluorine-containing ions increase in intensity with increasing collision energy (compare Figure 4a with 4b). It is also of particular interest that the fluorobenzene molecular ion picks up fluorine and CF_3 as well, although the ratio of relative intensities of the peaks m/z 114:113 ($[M+F-H_2]^{+\cdot}$ and $[M+F-H]^+$, respectively) is significantly greater than unity, in contrast to the m/z 96:95 ratio detected for the reaction of benzene molecular ion with the fluorinated surface.

Finally, we note that the peak at m/z 91 in the spectra obtained by using the fluorinated surface is due to the formal addition of CH to the benzene molecular ion. As

discussed above, this peak always appears in the benzene spectra obtained with hydrocarbon surfaces, so it may indicate the presence of hydrocarbons on the perfluorinated surface. The abundance of m/z 91 depends on the surface preparation. The lowest abundance of m/z 91 is detected when the fluorinated surface is prepared on plasma-cleaned vapor-deposited gold. A greater abundance of m/z 91 is observed when vapor-deposited gold is used with no plasma cleaning; a still greater abundance is observed when mechanically-polished gold foil is used. The ratio of the peaks m/z 91:96 increases slowly with time, suggesting that as the surface is damaged by F-removal, hydrocarbon is adsorbed. When the ion of m/z 91 becomes more abundant than m/z 95 or 96, the extent of fragmentation is still greater than that detected on a hydrocarbon surface.

Energetic considerations: fluorine addition

Unfortunately, the surface, and even one fluorinated chain (in our case e.g. Au-S-CH_2-CH_2-$(CF_2)_7$-CF_3), is too large for higher level *ab initio* calculations. Experimental heats of formation are also not available. It is well known, however, that longer chain monolayer films are oriented, ordered, crystalline structures.[21] In view of the hydrogen and CH_3, as well as the fluorine and CF_3 additions mentioned above, it is reasonable to assume that chemical reaction takes place between the projectile (e.g., benzene molecular ion) and the "uppermost" surface atoms or groups of the chain (in the case of the fluorinated surface, fluorine and CF_3). Therefore, it seems reasonable to model the surface by a smaller molecule, such as CF_3CF_3.

To enhance our understanding of the fluorine addition and the structures of the ions at m/z 96 and 95, we carried out quantum mechanical calculations on the above model system. Electronic wave functions were determined by applying the single-

configuration, self-consistent field, restricted Hartree-Fock (SCF) method[48] and, for closed-shell species, the 2nd order Møller-Plesset (MP2) perturbation method.[49] (The MP2 method was not available to us for open shell species). The following three basis sets were used: 3-21G,[50] 6-31G[51] and 6-31G*.[52] Geometries were optimized at the 6-31G SCF level with the symmetry restrictions given in Table 3. Total energies were also determined at the 6-31G SCF optimized geometries by the 6-31G* basis (referred as 6-31G*//6-31G SCF) and by the MP2 method (MP2 6-31G//6-31G SCF). Analytical second derivative calculations at the 6-31G SCF level proved to be computationally prohibitive for us, therefore zero point vibrational analyses were carried out at the 3-21G SCF level. For open-shell systems the restricted open-shell Hartree-Fock (ROHF) was applied. All *ab initio* calculations were performed using the program package GAMESS.[53] Due to the known limitations of the SCF method in energy calculations, we do not rely only on calculated total energies; available experimental heats of formation are also used in the following discussion.

Total energies obtained by 6-31G//6-31G, 6-31G*//6-31G SCF and MP2 6-31G//6-31G calculations, 3-21G zero point vibrational energies and experimental heats of formation of the investigated species are given in Table 3. To assist the reader, the experimental and SCF 6-31G*//6-31G relative energies for some processes are shown in Figure 6. Although the data given in Table 3 and shown in Figure 6 do not give us information on the transition states of the reactions, comparison of the (relative) energy levels can lead to some general conclusions.

According to the experimental heats of formation, the ionization of CF_3CF_3, and the accompanying the neutralization of the benzene molecular ion, is endothermic by 95.6 kcal/mol with respect to the reactants $C_6H_6^{+\cdot}$ and CF_3CF_3 (Figure 6). Simple loss of a

fluorine atom from the surface, i.e., a process without charge exchange, is predicted to be less favorable energetically by experimental heats of formation (by ca. 30 kcal/mol) than the charge exchange process. By analogy with the reaction of neutral benzene with F_2, which leads to ipso-fluorocyclohexadienyl radical,[54] i-$C_6H_6F^{\cdot}$ (denoted here by i-FCHD), it is reasonable to assume the formation of the corresponding ipso-cation in the surface collision process. Accordingly, the formation of i-FCHD cation is suggested to be less endothermic by calculations than the charge exchange process. The experimental heat of formation of this i-FCHD cation is not known; a value of 14.8+0.4 kcal/mol has been reported for the radical by Shobatake et al.[54] *Ab initio* 6-31G SCF energy results (Table 3) predict the ipso isomer to be less stable than "conventional" para and meta protonated fluorobenzenes (by about 15 and 8 kcal/mol),[55] but more stable than the F-protonated form (by about 19 kcal/mol). The losses of the H radical and the H_2 molecule from this i-FCHD cation are quite endothermic, by ca. 50 and 60 kcal/mol, respectively. This suggests that this cation, if it is formed by the collision, should contain a significant amount of internal energy for subsequent fragmentation. The almost similar endothermicity (or energy levels of the products, 101.8 and 111.2 kcal/mol, respectively; Fig. 6)) of H_2 and H loss from i-FCHD is in agreement with the experimentally found ca. 1:1 ratio of the peaks m/z 95:96. The appearance of the ion at m/z 95 in the 'reaction region' of the benzene SID spectra (Fig. 4) and, as well as in the normal mass spectrum and SID spectra (Fig. 5) of fluorobenzene, can also be attributed to the loss of H from the fluorobenzene molecular ion. However, in agreement with the low intensity of the $[M-H]^+$ peak in the fluorobenzene normal and SID spectra (Figure 5), this H loss from the fluorobenzene molecular ion is predicted to be highly endothermic by both experimental heats of formation (205.8-111.2=94.6 kcal/mol, Fig. 6) and *ab initio* 6-31G//6-31G and 6-

31G*//6-31G SCF calculations (203.2-98.6=104.6 kcal/mol, Fig. 6).[56]

According to the experimental heats of formation, the reaction of benzene molecular ion and fluorine radical can produce both the $C_6H_5F^+$ molecular ion and $C_6H_4F^+$ ions in slightly exothermic reactions (101.8-127.0=-25.2 kcal/mol and 111.2-127.0=-15.8 kcal/mol, respectively; Fig. 6). Therefore, it is reasonable to assume that this type of reaction might occur during the collision. Although the charge exchange is more favored energetically than the fluorine radical formation, the former 'neutralization' pathway can lead to fluorine addition only following an additional, very endothermic (using experimental heats of formation: 315.6-95.6=220 kcal/mol) elimination of F^+ cation.

Based on the data presented above, we suggest that the first step of the reaction of the molecular ion of benzene with the perfluorinated surface might be the abstraction of $F^{\cdot}$ radical from the surface and/or the formation of a high-energy content ipso-fluorocyclohexadienyl (i-FCHD) cation. Although the charge exchange process can not be excluded energetically, the high energy requirement of its subsequent step(s) suggests that the ions at m/z 95 and 96 are presumably not formed via this pathway. This mechanism contrasts with that proposed for methyl addition, which is suggested above, and in the literature,[17] to occur by an initial neutralization followed by transfer of an alkyl cation.

SID spectra of C_{60} with the fluorinated surface.

Both the benzene spectra reported here and the pyrazine spectra reported by Cooks[17] suggest that more internal energy is obtained by collision with a fluorinated surface than with a hydrocarbon surface (e.g., compare Figures 1 and 4). Buckminsterfullerene provides a challenging system for which the extent of fragmentation

can be explored on the two different types of surfaces. The early photodissociation studies of Smalley showed that fragmentation of C_{60}^+ occurred by multiple C_2 loss to yield ions as small as C_{32}^+, and further fragmentation beyond this point yielded even and odd number carbon cluster ions[37]. Initial gas-phase collision studies utilized kilovolt collisions with target gases such as He and O_2.[61-62] Successive loss of C_2 was observed[61], and in the case of collisions with O_2, kilovolt collisions were sufficient to fragment C_{60}^+ to yield small even and odd mass carbon fragments.[62] Heavier target gases, such as Xe, have been used to fragment C_{60}^+ at lower collision energies,[63-64] and loss of C_2 has been observed at collision energies near 150 eV using Xe under multiple collision conditions.[64] Several investigators have also studied collisions of fullerene ions with surfaces of various types. Whetten and coworkers have shown that C_{60}^+ is very stable toward fragmentation in surface collisions, and in their initial study they showed that no detectable fragmentation was observed at collision energies below 200 eV (using graphite and silicon surfaces).[15] At higher energies, successive C_2 loss was detected. Similar results have been reported by Hertel and coworkers in collisions of C_{60}^+ with graphite surfaces.[41] The absence of fragmentation in the surface collision experiments is consistent with the results of Smalley and coworkers,[37] where relatively high internal energy deposition (18 eV) was necessary to initiate for C_2 loss on a microsecond time scale.

Initial studies in our laboratory involved collisions of C_{60}^{2+} with a stainless steel surface.[40] It was found that the doubly-charged ion underwent charge reduction at the surface, and some fragmentation (yielding C_{54}^+, C_{56}^+ and C_{58}^+) was observed at a source-to-surface potential difference of 130 V (260 eV collision energy for the doubly-charged ion).[40] There was no detectable fragmentation of the singly-charged ion at

energies up to 130 eV. Investigations with other type of surfaces demonstrated that the composition of the surface has a distinct effect on the SID spectrum of C_{60}. For example, the SID spectra of doubly-charged buckminsterfullerene, C_{60}^{2+}, obtained by using octadecanethiol and fluorinated surfaces are shown in Figure 7. The behavior of C_{60}^{2+} in collisions with the octadecanethiol surface (Figure 7a) was similar to that observed with stainless steel. The primary feature of the spectrum is charge reduction; C_{60}^{+} is the major product. With collision energies of 190 eV, C_{56}^{+} and C_{58}^{+} can be observed, and at 210 eV, successive loss of 3 C_2 is observed. The threshold for C_2 loss appears to be similar to or only slightly lower than the threshold observed with stainless steel, consistent with the apparently similar energy deposition properties for both surfaces. Collisions of C_{60}^{+} with the octadecanethiol surface yielded no detectable fragmentation at collision energies of up to 160 eV. There was also a significant amount of ion signal appearing at low masses with collisions of both C_{60}^{+} and C_{60}^{2+}, which is attributed to (chemical) sputtering; the sputtering decreases in relative abundance with time.

Figure 7b shows the SID spectrum for a 250 eV collision of C_{60}^{2+} with the perfluorinated surface. The spectrum is characterized by significantly more fragmentation than was observed at similar energies on the stainless steel and octadecanethiol surface. For example, singly-charged fragment ions, corresponding to the loss of up to seven C_2 units (C_{46}^{+}), are observed. Moreover, doubly-charged fragment ions are also observed in the spectrum (fragments as small as C_{44}^{2+} are detected). The collision energy threshold for the appearance of C_2 loss also appeared to be significantly lower with the fluorinated surface; singly-charged fragments were detected at collision energies as low as 140 eV for collisions of C_{60}^{2+} with the perfluorinated surface. Fragments (C_{56}^{+} and C_{58}^{+}) were also detected in 160 eV collisions of C_{60}^{+} with the fluorinated surface. Finally,

lower abundances of chemical sputtering products were observed in collisions of C_{60}^{+} and C_{60}^{2+} with the fluorinated surface.

The effect of the surface composition on fullerene fragmentation behavior is manifested in two ways. The most direct effect of using the fluorinated surface is the appearance of the doubly-charged ion and its fragments in the SID spectrum. This can be attributed to the higher ionization potential for the fluorinated surface, as compared with that for either the octadecanethiol surface or hydrocarbon-covered stainless steel. The first ionization energy for C_{60} is known to be 7.6 eV.[65] There is some question as to the second ionization energy of C60, which has been variously measured to be 9.6 eV,[66] 10.2[67] and 12.6 eV,[68] depending on the technique employed. However, even the lowest estimate of the second ionization energy is considerably higher than the estimated ionization energies for either the octadecanethiol and stainless steel surfaces. Thus, significant reduction of the doubly-charged ion at the surface is expected, consistent with the observation that only singly-charged ions are observed as the products of collisions of C_{60}^{2+} with these surfaces. Similar arguments are expected to hold with regard to the neutralization of doubly-charged product ions formed near the surface. Since the ionization energies for fragments such as C_{58} are similar to those for C_{60}[65], it is likely that the resultant doubly-charged fragments will undergo some reduction. By contrast, the higher ionization energy for the fluorinated surface reduces the likelihood that charge reduction will occur when C_{60}^{2+} approaches the surface or when product ions are formed near the surface, with the resultant observation of reflected C_{60}^{2+} and its fragments. Of course, similar arguments can be made for C_{60}^{+} and its surface collision products. There is probably less neutralization of C_{60}^{+} and fragments in collisions with the fluorinated surface, which would improve the signal-to-noise ratio for the observation of products.

Improvements in signal-to-noise ratio could partially account for the observation of fragments at lower energies with the fluorinated surface.

As was the case with benzene, the fluorinated alkanethiol surface also appears to result in an increase in the translational-to-internal (t-i) energy transfer in surface collisions. This effect is difficult to separate entirely from the apparently higher signal-to-noise ratio for the formation of products from the fluorinated surface. Nevertheless, fragmentation is more extensive, and relative product abundance ratios are altered enough that the results are consistent with greater energy deposition at any given energy. For example, the ratio of C_{58}^+:C_{56}^+ resulting from a 210 eV collision of C_{60}^{2+} with the octadecanethiol surface is 3:1, while a 190 eV collision on the fluorinated surface results in a 1.1:1 C_{58}^+ to C_{56}^+ ratio. This effect is most likely due to a difference in energy deposition. Similar shifts have been observed in studies of gas-phase collisions of C_{60}^+. For example, in a study of collisions of C_{60}^+ with Xe (under multiple collision conditions in a triple quadrupole instrument), the C_{58}^+:C_{56}^+ ratio shifted from 3:1 to 1.2:1 as the collision energy was increased from 100 eV to 190 eV. Since lower energy collisions on the fluorinated surface produced a more nearly equal C_{58}^+:C_{56}^+ ratio (as compared to the octadecanethiol surface), it would appear that the energy transfer was higher on the fluorinated surface. However, because it has been observed that the formation of reaction products and their subsequent decomposition can play a role in the appearance of the spectrum (see discussion above), an increase in the energy transfer may not be the only explanation for the effect of the fluorinated surface.

The possibility that the fluorinated surface improves the relative translational-to-internal energy conversion raises a larger question: what is the actual energy transfer for an ion such as C_{60}^+? Previous estimates of the energy transfer for surface collisions of

small molecules have been on the order of 12-15%[1,9,16] and our preliminary results for $W(CO)_6$ on the fluorinated surface suggest conversion of about 20%.[69] However, Whetten and coworkers have estimated that translational-to-internal energy conversions are on the order of 25%-30% for large alkali halide clusters.[70] For C_{60}^+, these workers have estimated that 25% of the translational (t) collision energy is converted to internal (i) energy (based on studies of electron detachment from C_{60}^- in surface collisions) when C_{60} collides with a graphite surface.[15] This experimental estimate is consistent with a theoretical study by Mowrey and coworkers[71] in which a value of 25-30% was estimated from molecular dynamics simulations of collisions C_{60} with various surfaces. Hertel and coworkers have used similar energy conversion values to estimate internal energy deposition in collisions of C_{60}^+ with graphite[41]. Using their experimental data and unimolecular reaction rate theory, they have estimated a barrier height of roughly 10 eV for the loss of C_2 from C_{60}^+, a value thought to be consistent with the bond-breaking necessary to initiate loss of C_2. The results reported here show that with the fluorinated surface, fragmentation of C_{60}^+ can be observed with collisions of roughly 160 eV (which correlates with the onset of fragmentation for the doubly-charged ion as well). This is considerably lower than the energies at which fragmentation is observed in the experiments of Whetten and coworkers.[15] However, the ions in Whetten's experiments were formed by laser desorption and entrainment in a molecular beam, so they are internally cool and subsequent collisions did not involve a fluorinated surface. By contrast, the ions in our experiment are formed by a combination of thermal desorption and electron ionization and are internally hot before they collide with the fluorinated surface. It is therefore not surprising that they fragment at lower energies than in the Whetten[15] or Hertel[41] experiments (ions in the latter study probably have internal energies

intermediate between Whetten's study and our study).

The analysis of Hertel and coworkers[41] is useful in attempting to reconcile our results with the translational to internal (t-i) energy transfer in these experiments. Taking the case of 160 eV collisions of C_{60}^+ with the fluorinated surface, the fragment/parent ratio we observe is on the order 0.11. If it is assumed that ion flight times after the surface collision and activation are on the order of 10^{-5} s (activated ions travel a few centimeters at energies of roughly 10-20 eV before they are mass analyzed), the calculated rate constant is approximately 10^4 s^{-1} ($k=[\ln(1/0.9)]/10^{-5}$ s). Using RRKM theory[72-73], the unimolecular decay rate constant for the dissociation of an activated ion can be given approximately as:

$$k= \upsilon[(E-E_0)/E]^{s-1} \qquad (1)$$

where k is the rate constant, υ is the frequency factor, E_0 is the activation energy for C_2 loss, E is the internal energy, and s is the number of the available or active vibrations (assumed to be 3N-6 if all equal and participate in the reaction). Rather than use equation (1) to directly estimate the amount of internal energy deposition necessary to generate the measured rate constant, we have chosen to present the results in a way that reflects their inherent uncertainty. Given equation (1) above, plus an appropriately selected rate constant (e.g. in the range of 10^4-10^5 $s,^{-1}$) and an activation energy (E_0) of 10 eV (based on the estimate of the Hertel group[41]), a plot of the effective number of degrees of freedom vs. the amount of internal energy present in the activated ion can be prepared (Figure 8). Each line in the plot represents the number of degrees of freedom (y-axis) necessary to explain a given rate constant (e.g. $k= 10^4$ s^{-1} or 10^5) at the internal energy specified by the x-axis (for these calculations, υ was set to the value of 1×10^{13} s^{-1}); for lower values of υ, the slope of the plot will decrease). For C_{60}^+, if it is assumed

that energy is randomized among all 3n-7 modes (s-1=173), the expected internal energy deposition to generate rate constant of 10^4 s^{-1} is on the order of 80 eV. Can a calculated value of 80 eV be reconciled with the possible sources of internal energy for C_{60}^+ in this experiment? Since C_{60}^+ is formed by electron ionization of thermally desorbed (at 400 ^{0}C) buckminsterfullerene solid, it is reasonable to assume that the initial internal energy of the ions is at least 10 eV (from thermal desorption and from excess energy deposition during ionization). In fact, unimolecular dissociation is observed in the electron ionization mass spectrum of C_{60}^+; it is likely that some ions will have considerably higher internal energies than 10 eV. However, if it assumed that 10 eV is present initially, the remaining 70 eV must be deposited in the collision. In this particular case, the collision energy was 160 eV, suggesting that 44% of the translational energy was converted to internal energy. This is far higher than the 15% value used for small ions,[1,9,16] and higher than the 25-30% value estimated by Whetten and coworkers for C_{60}^+[14] although these estimates were not based on data for fluorinated surface.

There are several possible explanations for this unexpectedly high energy deposition. First, it may be the case that the effective number of oscillators in equation 1 is less than 3n-7. For example, if it assumed that 10 eV is initially present as internal energy, and that only 25% of the kinetic energy is converted to internal energy (40 eV), the effective number of oscillators is reduced to roughly 90. Such approximations have been used by a number of workers to explain variations between quasi-equilibrium theory (QET) and mass spectral data.[73] A second explanation for the calculated energy deposition figure may lie in an underestimate of the internal energy present in the ion prior to collision. Assuming that the effective number of oscillators is 173, and the energy deposition is 25% (40 eV), the initial internal energy would necessarily be on the order of

40 eV. It is probably reasonable to assume that some small fraction of the C_{60}^+ ions would possess this energy, but it is unclear whether the results can be fully explained by the initial internal energy. A third explanation is that the energy transfer is in fact higher for the fluorinated surface. The results presented above for benzene certainly support this hypothesis. This is particularly true if the effective number of oscillators in equation (1) can be assumed to be 173. In such a case, very high initial internal energies are necessary to explain efficiencies as low as 25% (much less 15%), and this would seem to be unlikely.

Clearly, there are a number of factors which influence an accurate estimate of the internal energy and the amount of t-i conversion during the surface collision. It is difficult to accurately determine the initial internal energy of C_{60}^+ in these experiments (although C_{60}^+ has certainly been prepared with lower initial internal energies by Whetten and coworkers)[15]. The initial rate constant estimate is subject to errors introduced in the estimation of fragment/parent ratio, and Figure 8 shows the effect of variations in the measured rate constant on the estimated internal energy deposition. The analysis presented here also assumes that the activation energy for C_2 loss is actually 10 eV. If the value is in fact lower, then slopes of the lines in Figure 8 will be greater and the estimated internal deposition will be lower. Nevertheless, the results presented here show that internal energy deposition is greater for the fluorinated surface than for stainless steel or octadecanethiol on gold and suggest that the translational-to-internal energy conversion is greater than 15%.

CONCLUSIONS

The results presented in this paper clearly show that, upon collision at kinetic

energies in the eV range, benzene reacts with hydrocarbon and fluorocarbon self-assembled monolayer films. Benzene serves as a useful "probe" molecule for the delineation of features of organized assemblies, giving different spectra for films prepared from long and short chain thiols. The transfer of translational-to-internal energy is much more effective for fluorinated alkanethiol films than for alkanethiol films. Several explanations, ranging from a simple classical mechanics description to a quantum mechanical description, can be offered. Two straightforward physical descriptions can be offered. Fluorine is larger than H, which may cause a greater momentum transfer, e.g., for collisions with the carbon of C_{60}^{2+}. Moreover, the greater rigidity of the fluorinated alkanethiol surface ("hard wall" rather than a "soft mattress"),[36] may lead to a smaller uptake of energy by the fluorinated surface compared with alkanethiol surface. The greater rigidity of the fluorinated surface can be attributed to enhanced repulsion between the more polar CF dipoles than between CH dipoles. The Massey parameter, the time of interaction between the incoming projectile and the surface compared with the period of motion being excited, might also be important. A more compressible surface should lead to a longer interaction or excitation time and greater transfer of vibrational energy to the surface. The greater electron density or partial negative charge of the fluorinated surface will result in a repulsive portion of the ion/surface interaction potential that rises more rapidly, and at shorter distances, than the potential surface associated with interaction between the ion and the alkanethiol surface. The interaction time at the fluorinated surface might, therefore, be lower than at the alkanethiol surface, resulting in greater electronic perturbation and higher energy deposition. Additional experiments, with a number of different projectile ions and surface types, are required to determine which of the above explanations, if any, most accurately describes the difference in

energy deposition between fluorocarbon and hydrocarbon surfaces.

EXPERIMENTAL

The experimental set-up has been described.[16] Two Extrel 4000u quadrupoles are positioned at 90° with a surface placed to intersect the ion optical path of the two quadrupoles. For the work presented here, ions were produced by 70 eV electron ionization. The surface can be rotated about the z-axis (Q1 and Q2 in the x-y plane). The surface is positioned 45-50° relative to the surface normal. The collision energy is varied by increasing the source potential relative to the surface potential; to transmit ions past the surface without collision, the potential difference is held at approximately 0 eV. The efficiency of the experiments is defined by $\Sigma_i I_i / \Sigma_j I_{trans}$, where $\Sigma_i I_i$ is the total ion current detected following collision (i.e., total scattered ion abundance detected) at a given collision energy and $\Sigma_j I_{trans}$ is the total parent ion current reflected past the surface without collision.

The alkane thiols were purchased from Aldrich (99%). The perdeuterated thiol was synthesized from the corresponding alkyl bromide ($C_{20}D_{41}Br$, Cambridge Isotope Laboratories; 97%D) and an equimolar amount of thiourea by a standard procedure (refluxing ethanol; hydrolysis with NaOH; acidification with H_2SO_4; extraction with benzene).[74] The fluorinated thiol was prepared from the corresponding iodide ($CF_3(CF_2)_7CH_2CH_2I$, Daikin Chemicals, Japan) and thiourea. Two types of surfaces were used in the experiments as indicated in the text. Gold foil (0.1 mm thick) was purchased from Aldrich and mechanically polished with alumina (starting with 1.0 μ and working down to 0.05μ alumina). The vapor-deposited gold surfaces were obtained from Evaporated Metal Films (Ithaca, NY). The surfaces are 17/32"x11/16" (0.5mm silica base)

and have an underlayer (50 Å) of either titanium dioxide or chromium that is covered with 1000 Å vapor-deposited gold. The surfaces were rinsed repeatedly in methanol and acetone followed by oxygen plasma cleaning for two hours. The surfaces were immediately immersed in a 20mM solution of a given thiol solution and is allowed to react for a minimum of 20 hours. In the text, the surfaces prepared from n-alkanethiols are referred to as hydrocarbon surfaces or are indicated by the number of carbons in the alkyl chain (e.g. C_{18}). The surface prepared from 2-(perfluorooctyl)-ethane thiol is referred to as the fluorinated surface.

A novel surface holder has been designed whereby four separate surfaces are aligned vertically, at the tip of a moveable probe, allowing any of the four surfaces to rest in the line of the ion beam. The holder is a 17/32"x3 1/4"x1/16" teflon strip with 0.5mm grooves to facilitate the surfaces. Individual stainless steel frames cover each surface, with a lead connecting all four frames to the voltage supply via the back of the holder. It is also possible to isolate each surface electrically and measure surface currents that may correlate to efficiency.

ACKNOWLEDGEMENTS. This work was supported, in part, by the Office of Naval Research and the Thomas F. and Kate Miller Jeffress Memorial Trust. We thank Julius Perel of Phrasor Scientific, Inc. (Duarte, CA) for the donation of the surface probe and vacuum lock.

REFERENCES

1. Cooks, R.G.; Ast, T.; Mabud, Md. A. *Int. J. Mass Spectrom. Ion Processes*, **1990**, *100*, 209.
2. Bier, M.E.; Schwartz, J.C.; Schey, K.L; Cooks, R.G. *Int. J. Mass Spectrom. Ion Processes*, **1990**, *103*, 1.
3. Schey, K.L.; Cooks, R.G.; Kraft, A; Grix, R.; Wollnik, H. *Int. J. Mass Spectrom. Ion Processes* **1989**, *94*, 1.
4. Ast, T.; Mabud, Md.A.; Cooks, R.G. *Int. J. Mass Spectrom. Ion Processes* **1988**, *82*, 131.
5. Hayward, M.J.; Mabud, Md.A.; Cooks, R.G. *J. Am. Chem. Soc.* **1988**, *110*, 1343.
6. Vincenti, M.; Cooks, R.G. *Org. Mass Spectrom.* **1988**, *23*, 317.
7. Bier, M.E.; Amy, J.W.; Cooks, R.G.; Syka, J.E.P; Ceja, P.; Stafford, G. *Int. J. Mass Spectrom. Ion Processes* **1987**, *77*, 331.
8. Mabud, MD.A.; DeKrey, M.J.; Cooks, R.G.; Ast, T. *Int. J. Mass Spectrom. Ion Processes* **1986**, *69*, 277.
9. DeKrey, M.J.; Kenttämaa, H.I.; Wysocki, V.H.; Cooks, R.G. *Org. Mass Spectrom.* **1986**, *21*, 193.
10. Mabud, Md. A.; DeKrey, M.J.; Cooks, R.G. *Int. J. Mass Spectrom. Ion Processes* **1985**, *67*, 285.
11. (a) Ijames, C.F.; Wilkins, C.L. *Anal. Chem.* **1990**, *62*, 1295.; (b) Williams, E.R.; Henry, K.D.; McLafferty, F.W.; Shabanowitz, J.; Hunt, D.F. *J. Am. Soc. Mass Spectrom.* **1990**, *1*, 413.
12. Aberth, W. *Anal. Chem.* **1990**, *62*, 609.
13. Cole, R.B.; LeMeilour, S.; Tabet, J.C. *Anal. Chem*, **1992**, *64*, 365.

14. Williams, E.R.; Jones, B.C., Jr.; Fang, L.; Zare,R.N.; Garrison, B.J.; Brenner, D.W. *J. Am. Chem. Soc.*, **1992**, *114*, 3207.

15. Beck, R.D.; St. John, P.; Alvarez, M.M.; Diederich, F.; Whetten, R.L. *J. Phys. Chem.* **1991**, *95*, 8402.

16. Wysocki, V.H.; Ding, J.-M.; Jones, J.L.; Callahan, J.H.; King, F.L. *J. Am. Soc. Mass Spectrom.*, **1992**, *3*, 27.

17. B.E. Winger, R.K. Julian, Jr., R.G. Cooks, C.E.D Chidsey *J. Am. Chem. Soc.*, **1991**, *113*, 8967.

18. V.H. Wysocki, J.L. Jones, J.-M. Ding *J. Am. Chem. Soc.*, **1991**, *113,* 8969.

19. Porter, M.D.; Bright, T.B.; Allara, D.L.; Chidsey, C.E.D. *J. Am. Chem. Soc.* **1987**, *109*, 3559.

20. Strong, L.; Whitesides, G.M. *Langmuir*, **1988**, *4*, 546.

21. Bain, C.D.; Troughton, E.B.; Tao, Y.-T.; Evall, J.; Whitesides, G.M.; Nuzzo, R. *J. Am. Chem. Soc.* **1989**, *111*, 321.

22. Nuzzo, R.G.; Dubois, L.H.; Allara, D.L. *J. Am. Chem. Soc.* **1990**, *112*, 558.

23. Whitesides, B.M.; Laibinis, P.E. *Langmuir*, **1990**, *6*, 87.

24. Bryant, M.A.; Pemberton, J.E. *J. Am. Chem. Soc.* **1991**, *113*, 3629.

25. Alves, C.A.; Smith, E.L.; Porter, M.D. *J. Am. Chem. Soc.* **1992**, *114*, 1222.

26. Chidsey, C.E.D.; Loiacono, D.N. *Langmuir* **1990**, *6*, 682-691.

27. Chidsey, C.E.D.; Bertozzi, C.R.; Putvinski, T.M; Myjsce, A.M. *J. Am. Chem. Soc.* **1990**, *112*, 4301.

28. Li, T. T.-T.; Weaver, M.J. *J. Am. Chem. Soc.* **1984**, *106*, 6107.

29. Rubenstein, I.; Steinberg, S.; Tor, Y.; Shanzer, A.; Sagiv, J. *Nature* **1988**, *332*, 426.

30. Finklea, H.O.; Avery, S.; Lynch, M. *Langmuir*, **1987**, *3*, 409.

31. Finklea, H.O.; Snider, D.A.; Fedyk, J. *Langmuir* **1990**, 6, 371.

32. Finklea, H.O; Hanshew, D.D. *J. Am. Chem. Soc.* **1992**, *114*, 3173.

33. Swalen, J.D.; Allara, D.L.; Andrade, J.D.; Chandross, E.A.; Garoff, S.; Israelachvili, J.; McCarthy, T.J.; Murray, R.; Pease, R.F.; Rabolt, J.F.; Wynne, K.J.; Yu, H. *Langmuir* **1987**, *3*, 932.

34. (a) Nuzzo, R.G.; Allara, D.L.; *J. Am. Chem. Soc.* **1983**, *105*, 4481. (b) Allara, D.L.; Nuzzo, R.G. *Langmuir* **1985**, *1*, 45.

35. Tillman, Y.N.; Ulman, A.; Penner, T.L. *Langmuir* **1989**, *5*, 101.

36. Cohen, S. R.; Naaman, R., Sagiv, J. *Phys. Rev. Lett.* **1987**, *58*, 1208.

37. O'Brien, S.C.; Heath, J.R.; Curl, R.F.; Smalley, R.E. *J. Chem. Phys.* **1988**, **88**, 220.

38. Krätschmer, W.; Lamb, L.D.; Fostiropoulos, K.; Huffman, D.R. *Nature* **1990**, **347**, 354.

39. For a recent review of this subject see: McElvany, S.W.; Ross, M.M. *J. Am. Soc. Mass Spectrometry* **1992**, *3*, 268-280.

40. (a) McElvany, S.W.; Ross, M.M.; Callahan, J.H. *Mat. Res. Soc. Proc.* **1991**, *206*, 697-702; (b) Callahan, J.H.; Ross, M.M.; Wysocki, V.H. *Proc. 39th ASMS Conf. Mass Spectrometry and Allied Topics* Nashville, TN, May 19-24, **1991**, 829-830.

41. (a) Busmann, H.-G.; Lill, Th.; Reif, B.; Hertel, I.V. *Surface Science*, in press, **1992**. (b) Campbell, E.E.B.; Hielscher, A.; Ehlich, R.; Hertel, I.V. *Proc. of the 88th Heraeus Seminar*, in press, **1992**.

42. Rosenstock, H.M.; Dannacher, J.; Liebman, J.F. *Radiat. Phys. Chem.* **1982**, *20*, 7.

43. An ion of m/z 27 could also consist of C_2DH but the analogous product, C_2H_2, is of low relative abundance in the surface collision spectrum of $C_6H_{6+\cdot}$.

44. Gross, M.L. Russell, D.H.; Aerni, R.J. Bronczyk *J. Am. Chem. Soc.* **1977**, *99*, 36xx.

45. ΔH_f (experimental): C_6H_6, 19.8; $C_6H_6^{+\cdot}$, 233; $C_6H_7^+$ 204 (PA benzene 181.3); $C_6H_5^+$ 272.8; H, 52.0; H_2, 0.

46. An ion of M/Z 43 could also have the molecular formula C_2H_3O: In your data, $C_3H_7^+$ seems more likely because larger alkyl ions C_nH_{2n+1} and their dissociation products CnH_{zn-1} and CnH_{zn-3} are often detected.

47. Lias, S.G.; Bartmess, J.E.; Liebman, J.F.; Holmes, J.L.; Levin, R.D.; Mallard, W.G. *J. Phys. Chem. Ref. Data*, **1988**, *17*, Suppl. 1.

48. Binkley, J. S.; Pople, J. A.; Dobosh, P. A. *Mol. Phys.* **1974**, *28*, 1423.

49. Carsky, P.; Hess, B. A., Jr.; Schaad, L. J. *J. Comput. Chem.* **1984**, *5*, 280 and references therein.

50. Binkley, J. S.; Pople, J. A.; Hehre, W. J. *J. Am. Chem. Soc.* **1980**, *102*, 939.

51. Hehre, W. J.; Ditchfield, R.; Pople, J. A. *J. Chem. Phys.* **1972**, *56*, 2257.

52. Pietro, W. J.; Francl, M. M.; Hehre, W. J.; DeFrees, D. J.; Pople, J. A.; Binkley, J. S. *J. Am. Chem. Soc.* **1982**, *104*, 5039.

53. Schmidt, M. W.; Baldridge, K. K.; Boatz, J. A.; Jensen, J. A.; Koseki, S.; Gordon, M. S.; Nguyen, K. A.; Windus, T. L.; Elbert, S. T. Program Package GAMESS, *QCPE Bulletin*, **1990**, *10*, 52.

54. Grover, J.; Wen, Y.; Lee, Y. T.; Shobatake, K. *J. Chem. Phys.* **1988**, *89*, 938.

55. Bader, R. F. W.; Chang, C. *J. Phys. Chem.* **1989**, *93*, 5095.

56. We note here that we used the 6-31G*//6-31G energy value obtained for the para-C_6H_4F isomer in the above discussion, which was found to be the most stable isomer by STO-3G[57], 6- 31G//6-31G and 6-31G*//6-31G SCF calculations.

Although MP2 6-31G//6-31G SCF calculations predict the meta isomer to be slightly more stable than the para isomer, the small energy difference (0.3 kcal/mol) between these isomers shows that the selection of the para-C_6H_4F isomer has no significant effect on our conclusions. To estimate the error on energy calculation caused by the application of 6-31G equilibrium geometry, we carried out 6-31G* SCF geometry optimization on the i-FCHD cation. The 6-31G*//6-31G* SCF energy of this ion is calculated to be lower by only 0.3 kcal/mol than that of the 6-31G*//6-31G SCF energy. Assuming C_s symmetry, which proved to be minimum by 3-21G zero point vibrational energy (ZPVE) calculation, the benzene ring is calculated to be almost planar with the torsion angle C_1-C_2-C_3-C_4 of 8.5 degrees in this ipso-cation, i-FCHD. Both the fluorine and hydrogen atoms are 'normally' bonded, so the structure is a σ-complex type structure rather than that of a 'loosely bonded' $[C_6H_6...HF]^{+\cdot}$ complex.

57. Dill, J. D.; Schleyer, P. v. R.; Pople, J. A. *J. Am. Chem. Soc.* **1977**, *99*, 1.

58. Leung, H-W.; Harrison, A. G. *J. Am. Chem. Soc.* **1979**, *101*, 3168.

59. Schmidt, M. W.; Ruedenberg, K. *J. Chem. Phys.* **1979**, *71*, 3951.

60. Herzberg, G. *J. Mol. Spectrosc.* **1970**, *33*, 147.

61. Young, A.B.; Cousins, L.; Harrison, A.G. *Rapid Comm. Mass Spectrom.* **1991**, *5*, 226.

62. Doyle, R.J., Jr.; Ross, M.M. *J. Phys. Chem.* **1991**, *95*, 4954.

63. Ben-Amotz, D.; Cooks, R.G.; Dejarme, L.; Gunderson, J.C.; Hoke, S.H.; Kahr, B.; Payne, G.L.; Wood, J.M. *Chem. Phys. Lett.* **1991**, *183*, 149.

64. McElvany, S.W.; Callahan, J.H. *J. Phys. Chem.* **1991**, *95*, 6186.

65. Zimmerman, J.A.; Eyler, J.R.; Bach, S.B.H.; McElvany, S.W. *J. Chem. Phys.* **1991**,

94, 3556.

66. Steger, H.; de Vries, J.; Kamke, B.; Kamke, W.; Drewello, T. *Chem. Phys. Lett.* **1992**, submitted.

67. Caldwell, K.A.; Giblin, D.E.; Gross, M.L. *J. Am. Chem. Soc.* **1992**, *114*, 3743.

68. Lifshitz, C.; Iraqi, M.; Peres, T.; Fischer, J. *Rapid Comm. Mass Spectrom.* **1991**, *5*, 238.

69. Kane, T.E.; Somogyi, A.; Wysocki, V.W.; unpublished results.

70. Beck, R.D.; St. John, P.; Homer, M.L.; Whetten, R.L. *Science* **1991**, *253*, 879.

71. Mowrey, R.C.; Brenner, D. W.; Dunlap, B.I.; Mintmire, J.W.; White, C.T. *J. Phys. Chem.* **1991**, *95*, 7138.

72. Rice, O.K.; Ramsperger, H.L. *J. Am. Chem. Soc.* 1927, **49**, 1617, Kassel, L.S. *J. Chem. Phys.* 1928, **32**, 225.

73. Robinson, P.J.; Holbrook, K.A. Unimolecular Reactions Wiley-Interscience, New York, 1972, pp. 52-63.

74. Urquhart, G.G.; Gates, J.W., Jr.; Connor, R. *Org. Synth., Coll. Vol. III*, **1955**, 363.

Table 1. Major dissociation products expected from ionized benzene, $C_6H_6^{+\cdot}$ (m/z 78) and ionized benzene-d_6, $C_6D_6^{+\cdot}$ (m/z 84).

$C_6H_6^{+\cdot}$		$C_6D_6^{+\cdot}$	
m/z	Formula	m/z	Formula
27	C_2H_3	30	C_2D_3
39	C_3H_3	42	C_3D_3
50	C_4H_2	52	C_4D_2
51	C_4H_3	54	C_4D_3
52	C_4H_4	56	C_4D_4
53	C_4H_5	58	C_4D_5
63	C_5H_3	66	C_5D_3
77	C_6H_5	82	C_6D_5

Table 2. Relative abundance of selected fragment ions detected when ionized benzene is allowed to collide with stainless steel (SS) or self-assembled monolayer films prepared from n-alkanethiols containing 2, 3, 4, 10, or 18 carbons.

m/z	SS	C_2	C_3	C_4	C_{10}	C_{18}
105	0.0	0.4	0.3	0.3	0.3	0.1
103	0.2	0.5	0.3	0.3	0.4	0.1
91	5.2	5.8	4.7	5.7	6.2	6.9
89	0.2	0.2	0.2	0.2	0.2	0.5
79	16.6	19.2	18.9	19.6	18.2	13.2
78	60.1	60.0	53.8	55.1	51.3	**100.0**
77	**100.0**	**100.0**	**100.0**	**100.0**	**100.0**	59.2
65	5.1	5.2	4.0	4.6	4.9	4.1
63	6.5	7.2	6.2	6.2	5.4	4.3
57	1.3	0.8	0.7	0.6	0.8	0.0
53	18.2	19.9	16.7	16.7	16.4	7.3
52	51.5	56.6	50.1	51.3	46.7	41.1
51	34.2	40.2	35.1	36.6	35.4	12.6
50	7.0	7.9	6.9	6.8	5.9	4.0
43	2.2	2.7	1.9	2.1	2.2	0.1
39	34.1	38.4	32.2	32.8	31.5	20.1
38	0.4	0.9	0.7	0.8	0.6	0.3
27	17.7	19.1	14.4	14.7	14.8	3.7
26	0.7	1.0	0.7	0.8	0.7	0.2

Figure Captions

Figure 1. SID mass spectra obtained by colliding benzene molecular ion at (**a**) 30 eV and (**b**) 70 eV collision energies with a surface prepared from n-octadecanethiol on vapor-deposited gold.

Figure 2. SID mass spectra in the methyl reaction region obtained by 30 eV collisions of (**a**) benzene molecular ion with a surface prepared from n-$C_{20}D_{41}SH$, (**b**) benzene-d_6 molecular ion with a surface prepared from n-$C_{18}H_{37}SH$, and (**c**) benzene-d_6 with a surface prepared from n-$C_{20}D_{41}SH$ (all on vapor-deposited gold).

Figure 3. SID mass spectra obtained by colliding benzene molecular ion at (**a**) 30 eV and (**b**) 70 eV collision energies with a surface prepared from n-decanethiol on vapor-deposited gold.

Figure 4. SID mass spectra obtained by colliding benzene-d_6 molecular ion at (**a**) 30 eV and (**b**) 70 eV collision energies with a surface prepared from 2-(perfluorooctyl)-ethanethiol on vapor-deposited gold.

Figure 5. SID mass spectra obtained by colliding fluorobenzene molecular ion at 30 eV collision energies with a surface prepared from 2-(perfluorooctyl)-ethanethiol on vapor-deposited gold.

Figure 6. Relative energies of some of the possible products of the reaction between benzene molecular ion and CF_3CF_3. All values are in kcal/mol; exp and SCF denote

values obtained by using experimental heats of formation and 6-31G*//6-31G SCF total energies (and the Hartree-Fock limit value, 0.5 hartree, for hdyrogen atom and experimentally determined energy, -1.174 hartree, for H_2 molecule) given in Table 3, respectively. (*Based on 6-31G//6031G SCF energies.)

Figure 7. Mass spectra obtained by 250 eV collisions of C_{60}^{++} with surfaces prepared from (**a**) n-octadecanethiol and (**b**) 2-(perfluorooctyl)-ethanethiol on vapor-deposited gold.

Figure 8. Representation of the effective number of oscillators of C_{60}^{+} needed to achieve dissociation rates of 10^4 s^{-1} (solid line) or 10^5 s^{-1} (dashed line), given E_0=10 eV and $\upsilon=1x10^{13}$.

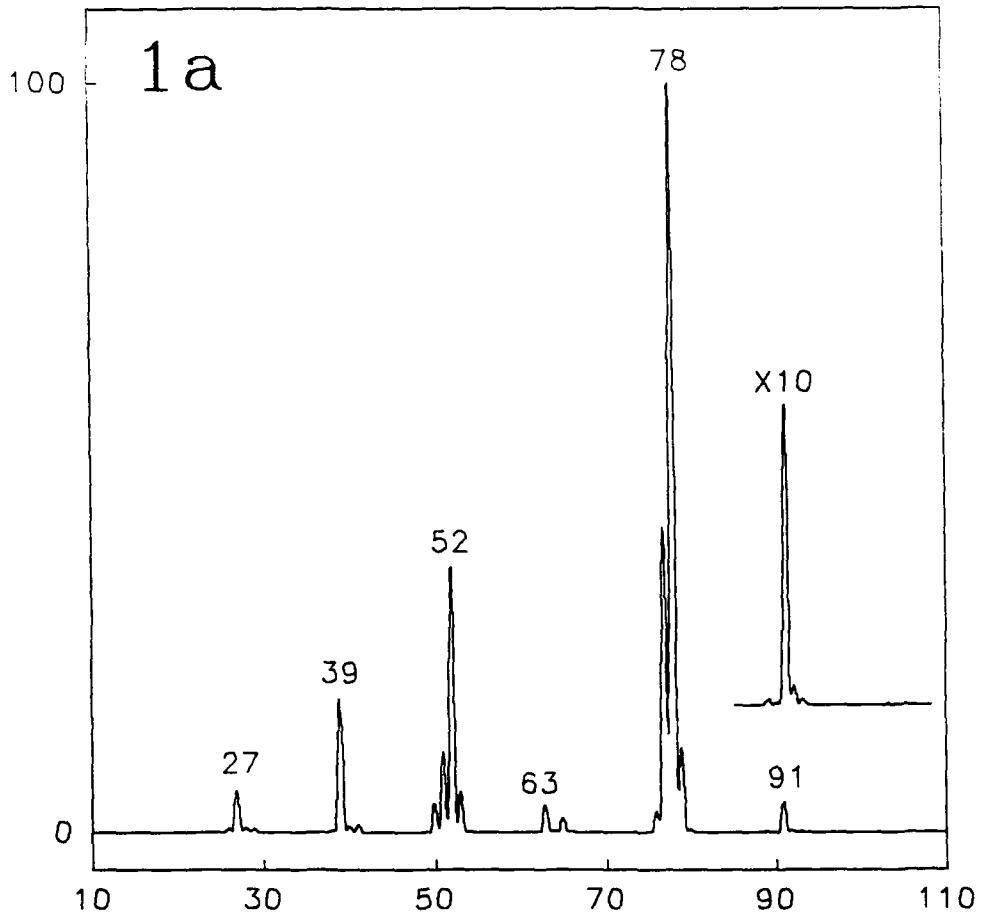
1a
100
0
78
X10
52
39
27
63
91
10
30
50
70
90
110

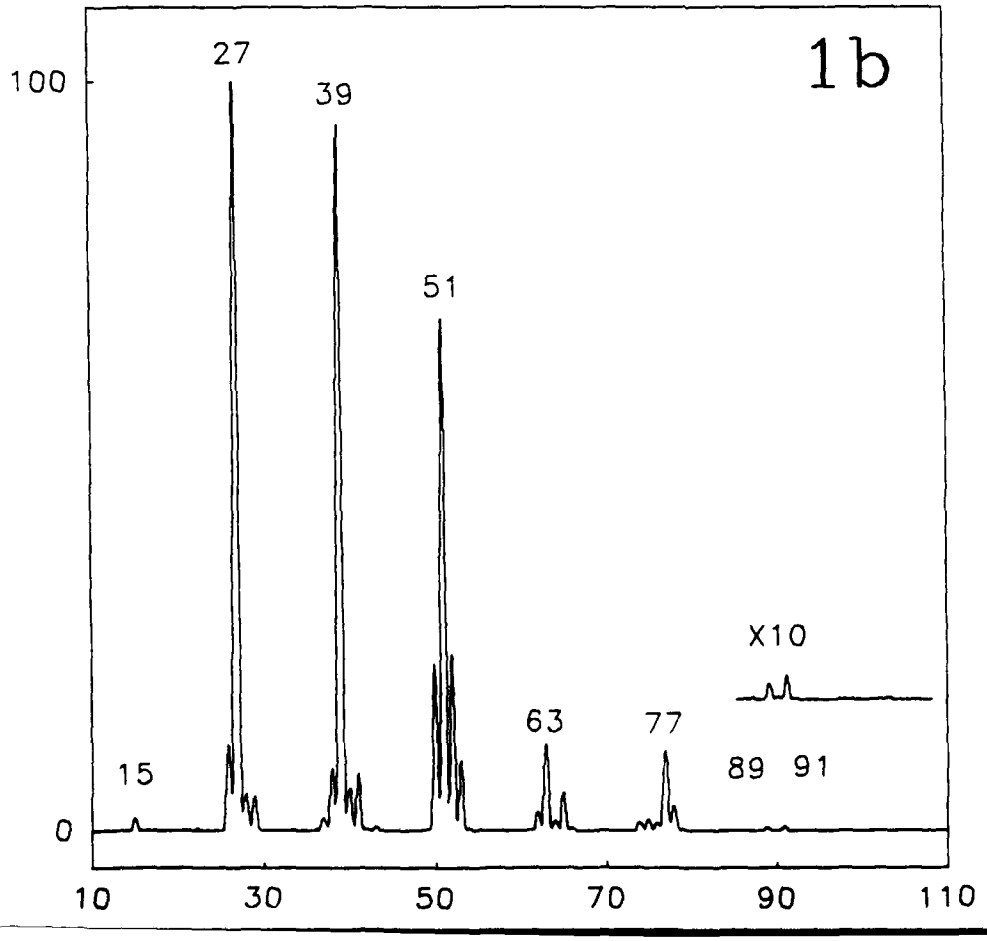
1b
100
0
27
39
51
X10
63
77
15
89
91
10
30
50
70
90
110

Fig. 2

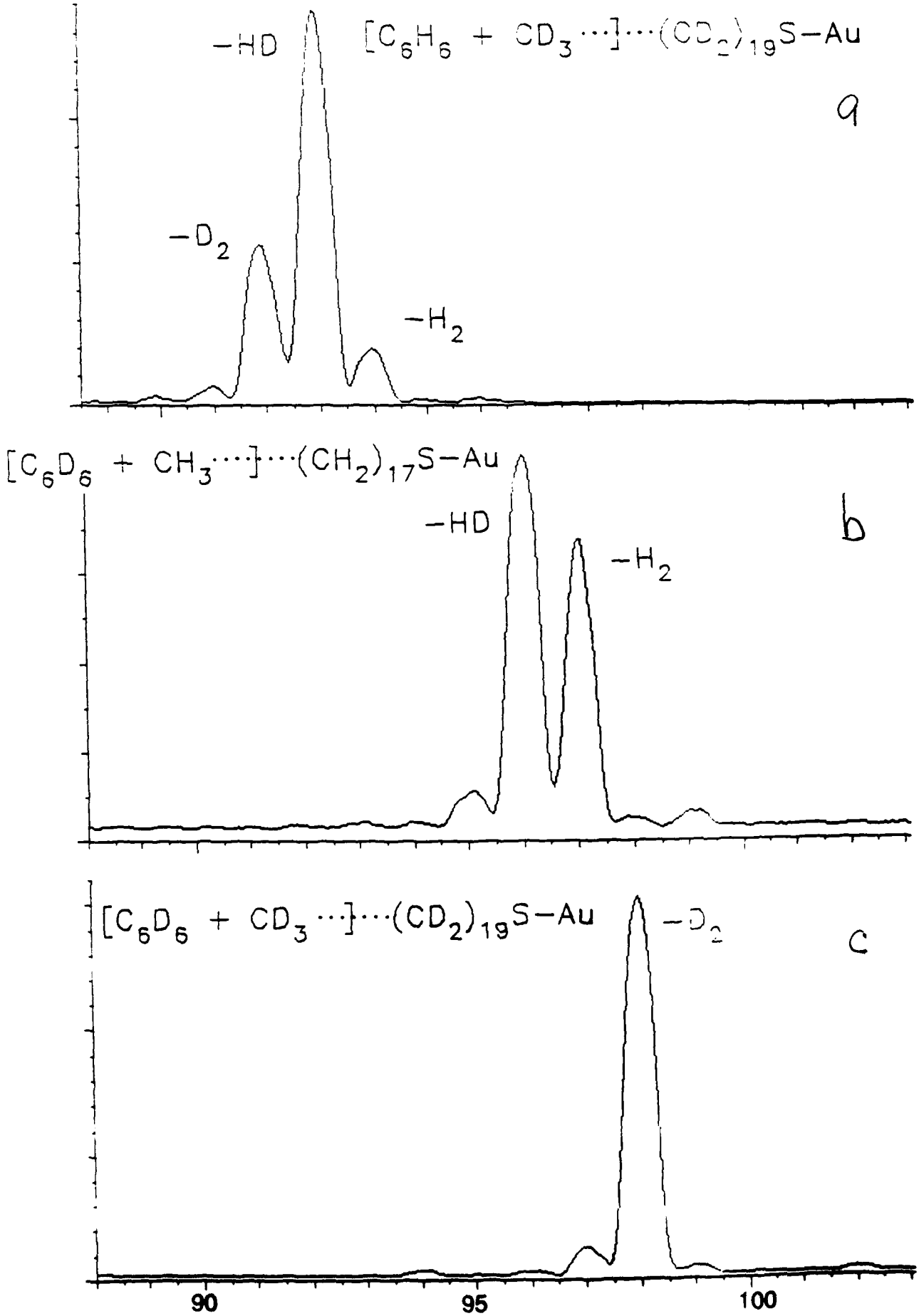
−HD
[C6H6 + CD3···]···(CD2)19S−Au
a
−D2
−H2
[C6D6 + CH3···]···(CH2)17S−Au
−HD
−H2
b
[C6D6 + CD3···]···(CD2)19S−Au
−D2
c
90
95
100

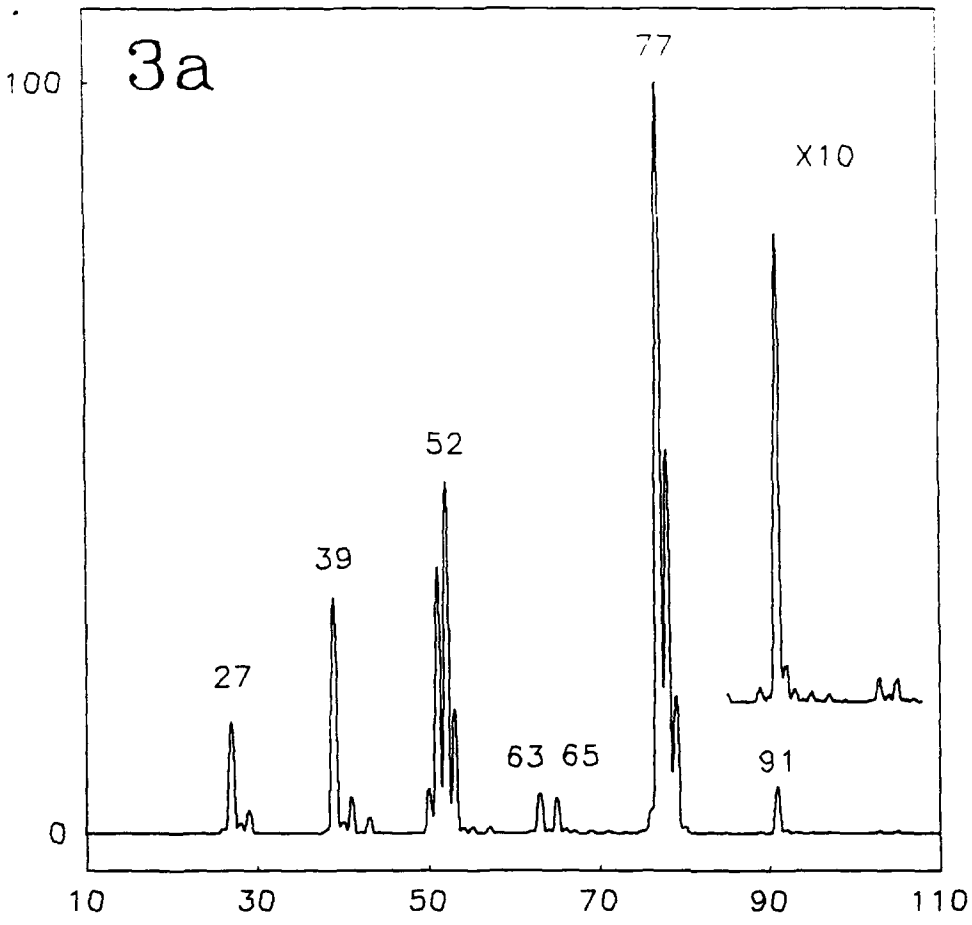
3a
100
0
77
X10
52
39
27
63 65
91
10
30
50
70
90
110

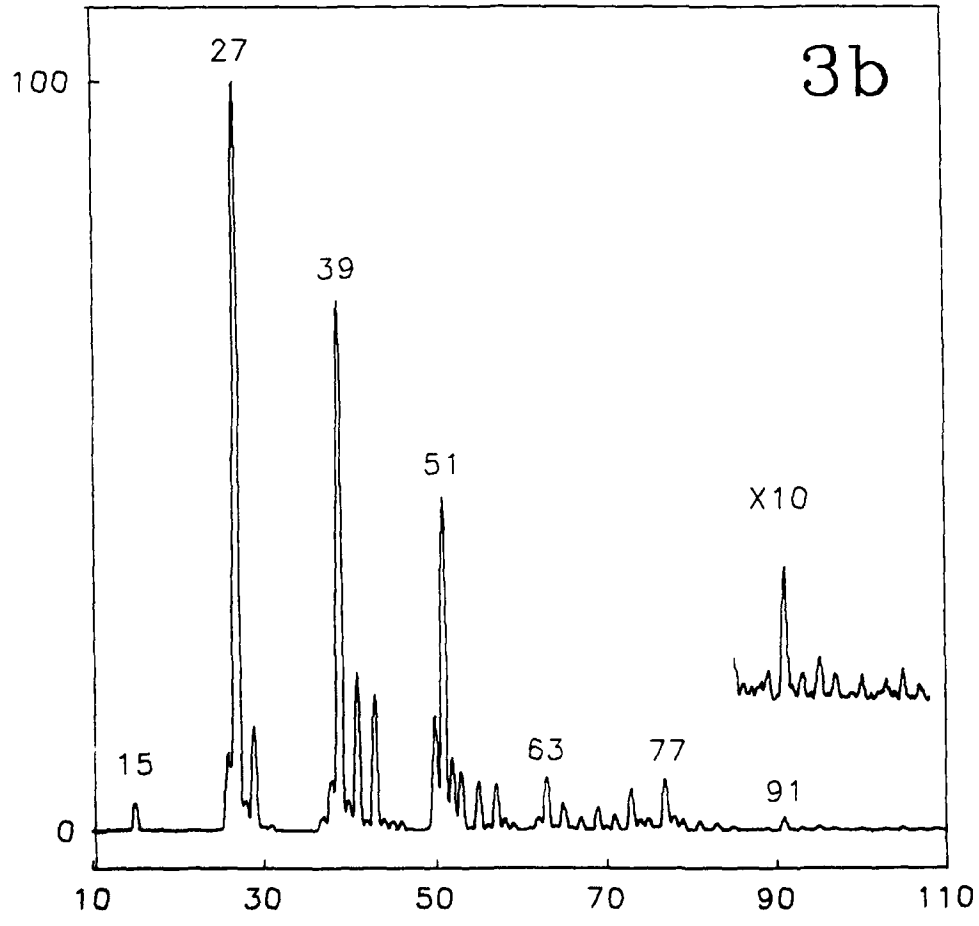
3b
100
0
27
39
51
X10
15
63
77
91
10
30
50
70
90
110

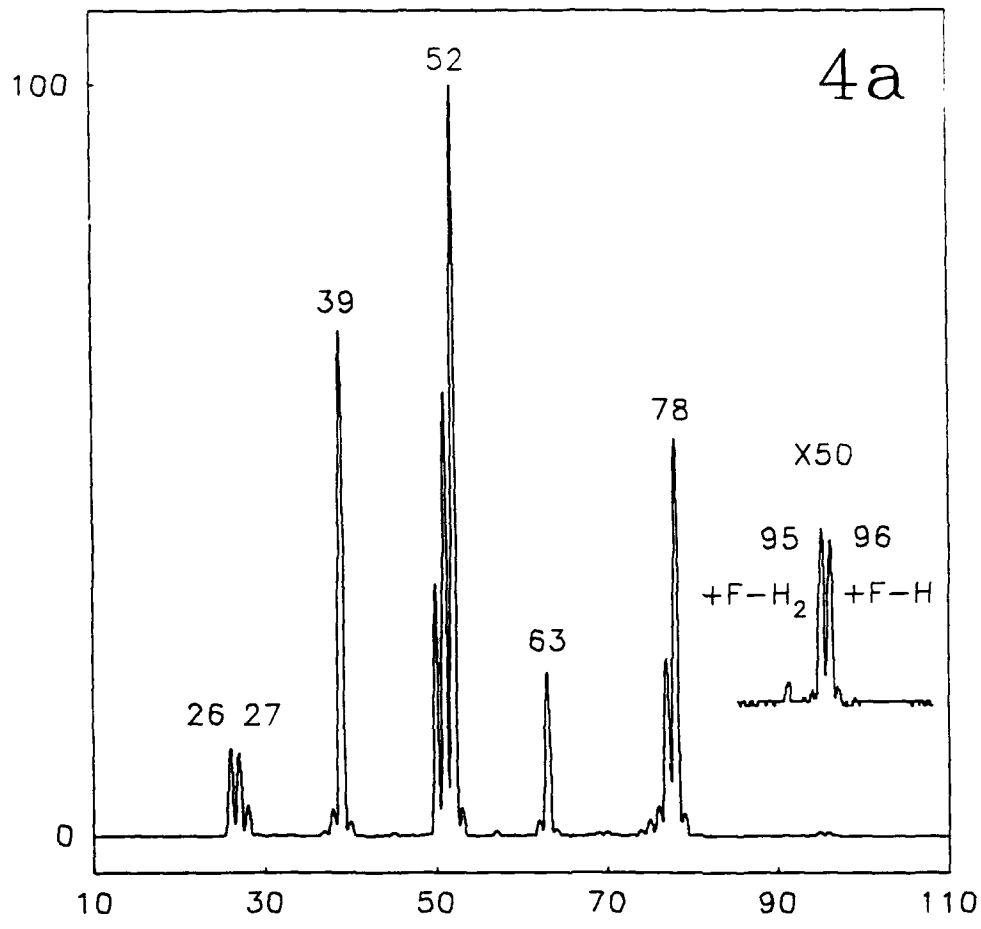
4a
100
0
52
39
78
63
26 27
X50
95
96
+F−H2
+F−H
10
30
50
70
90
110

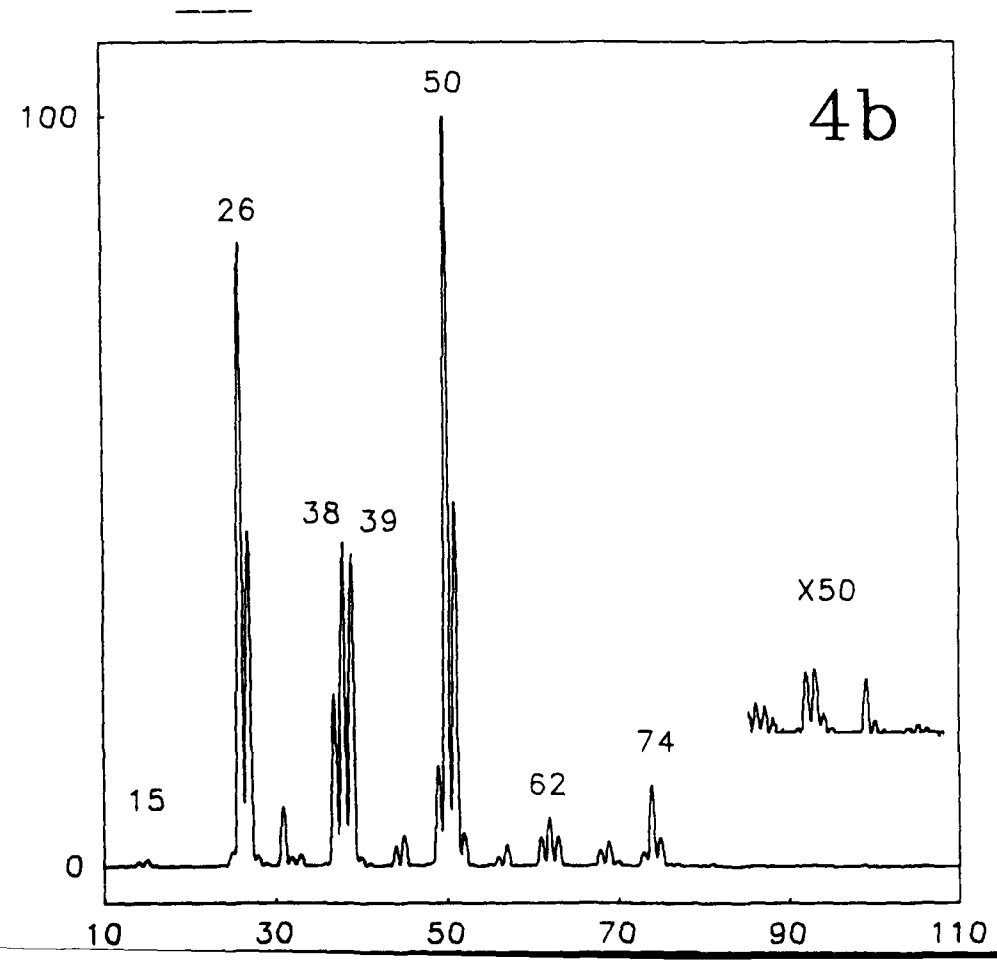
4b
100
0
50
26
38 39
15
62
74
X50
10
30
50
70
90
110

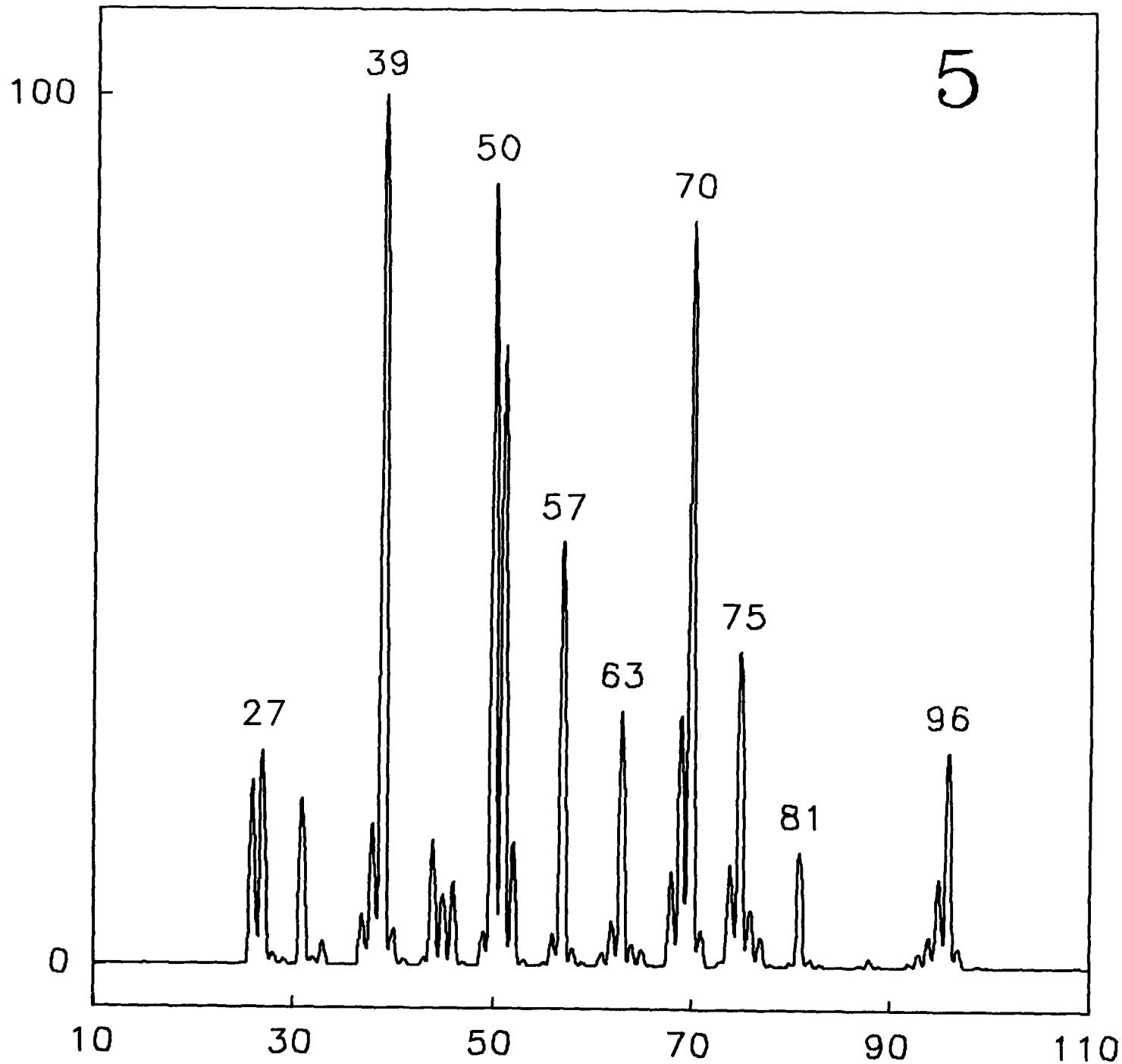
5
100
0
39
50
70
57
75
63
27
96
81
10
30
50
70
90
110

Fig. 6

exp.:315.6; SCF:364.2

exp.:205.8; SCF:203.2

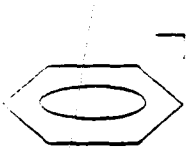

exp.:127.0; SCF:90.3

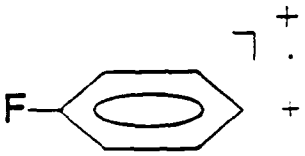

exp.:111.2; SCF:98.6

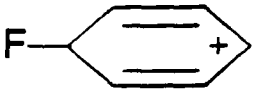

exp.:101.8; SCF:94.0

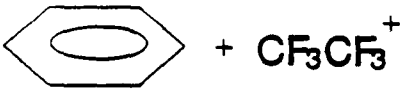

exp.:95.6; SCF:135.2*

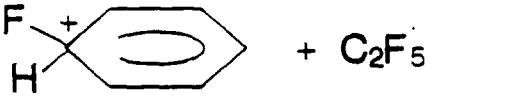

SCF: 50.5

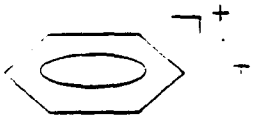

exp.: 0.0; SCF: 0.0

SCF
6-31G*//6-31G SCF
*6-31G//6-31G SCF

Fig 7

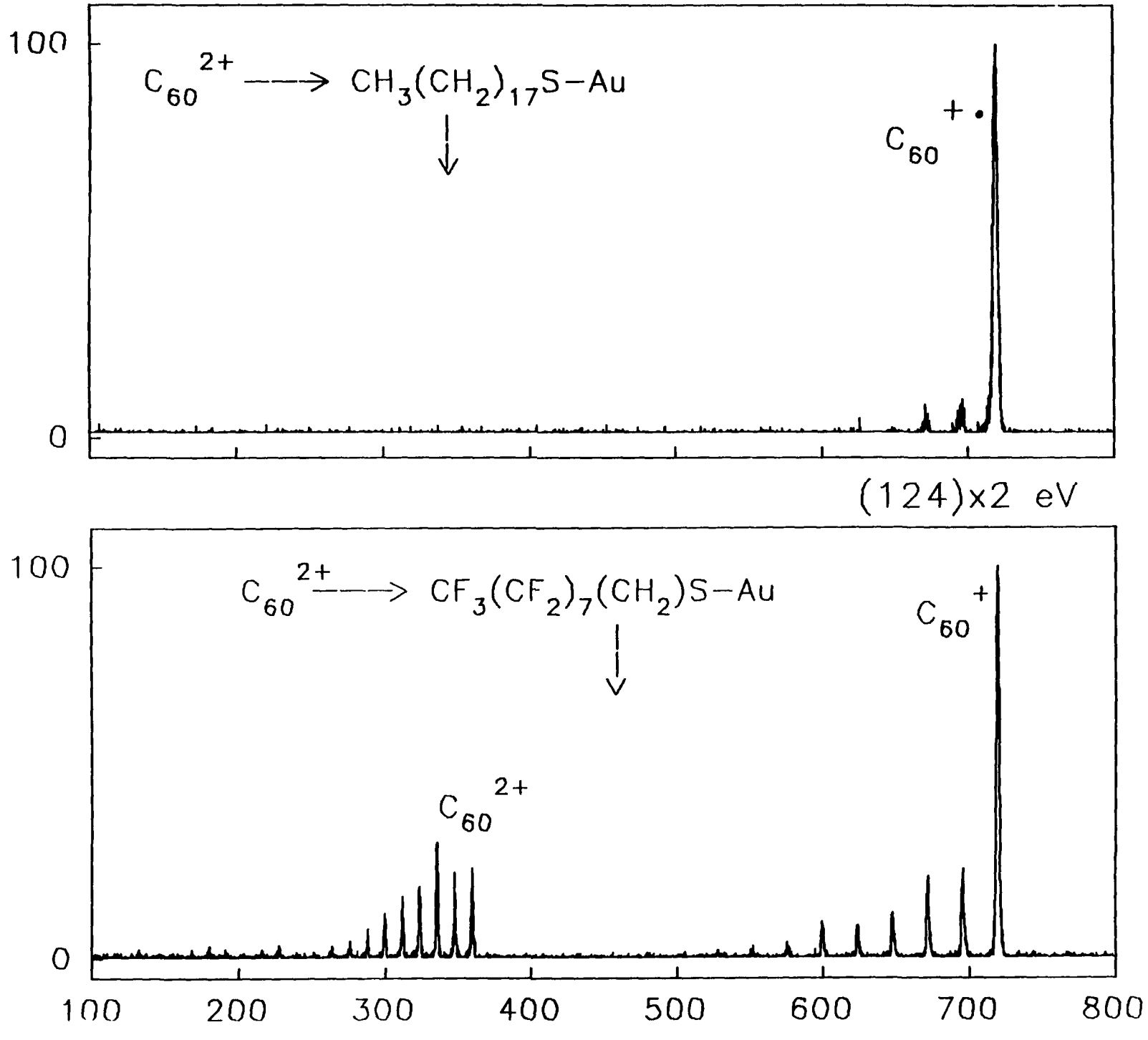
a
100
$C_{60}^{2+} \longrightarrow CH_3(CH_2)_{17}S-Au$
$C_{60}^{+\bullet}$
0
(124)x2 eV
b
100
$C_{60}^{2+} \longrightarrow CF_3(CF_2)_7(CH_2)S-Au$
C_{60}^{+}
C_{60}^{2+}
0
100
200
300
400
500
600
700
800

Fig 8

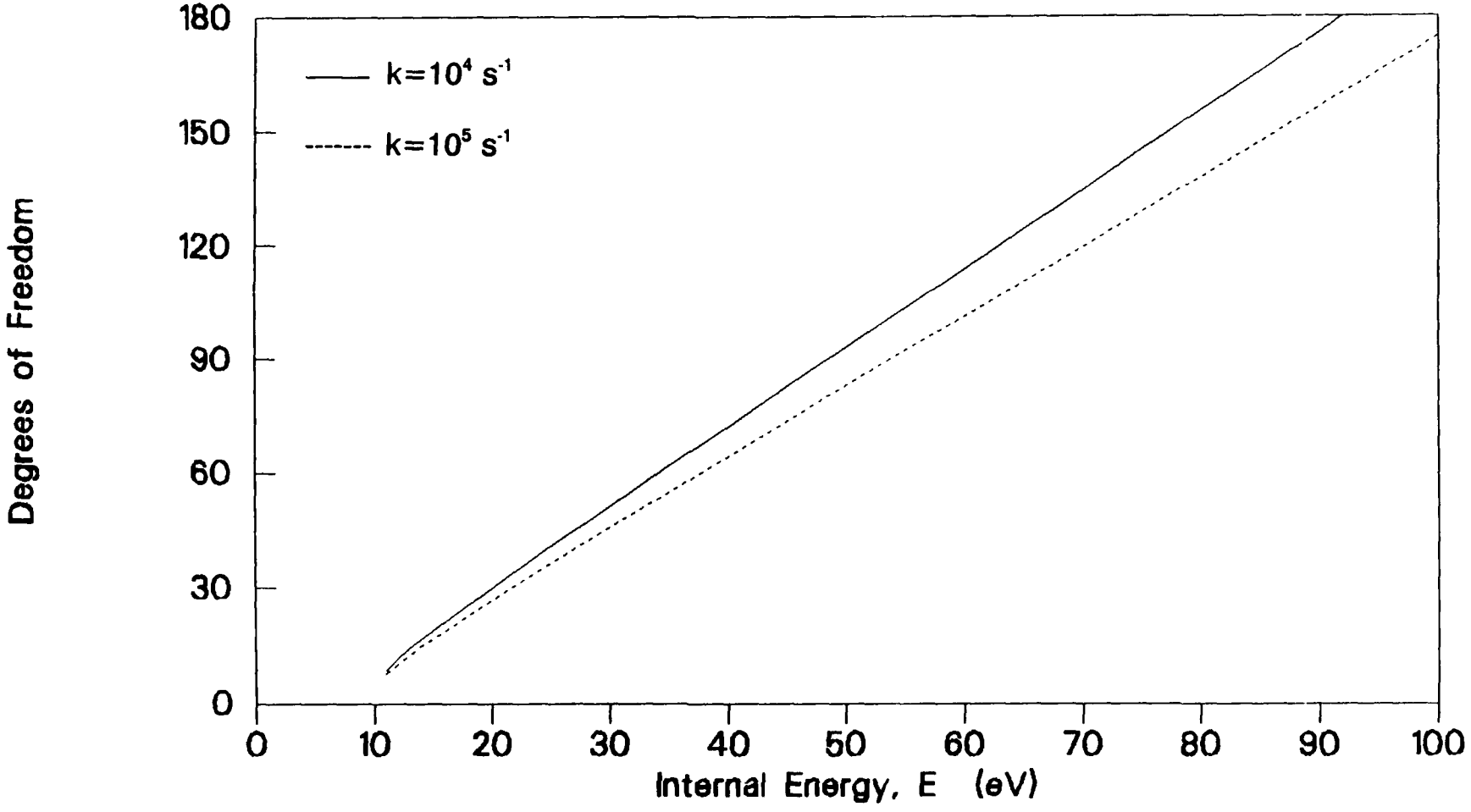
Degrees of Freedom
180
150
120
90
60
30
0
k=10⁴ s⁻¹
k=10⁵ s⁻¹
0
10
20
30
40
50
60
70
80
90
100
Internal Energy, E (eV)